
Learning Transferable Sensor Models via Language-Informed Pretraining

Yuliang Chen¹ Arvind Pillai¹ Yu Yvonne Wu¹ Tess Z. Griffin¹ Lisa Marsch¹ Michael V. Heinz¹
 Nicholas C. Jacobson¹ Andrew Campbell¹

Abstract

Modern sensing systems generate large volumes of unlabeled multivariate time-series data. This abundance of unlabeled data makes self-supervised learning (SSL) a natural approach for learning transferable representations. However, most existing approaches are optimized for reconstruction or forecasting objectives and often fail to capture the semantic structure required for downstream classification and reasoning tasks. While recent sensor–language alignment methods improve semantic generalization through captioning and zero-shot transfer, they are limited to fixed sensor configurations, such as predefined channel sets, signal lengths, or temporal resolutions, which hinders cross-domain applicability. To address these gaps, we introduce **SLIP** (Sensor Language-Informed Pretraining), an open-source framework for learning language-aligned representations that generalize across diverse sensor setups. SLIP integrates contrastive alignment with sensor-conditioned captioning, facilitating both discriminative understanding and generative reasoning. By repurposing a pretrained decoder-only language model via cross-attention and introducing an elegant, flexible patch-embedder, SLIP supports different temporal resolutions and variable-length input at inference time without additional retraining. Across 11 datasets, SLIP demonstrates superior performance in zero-shot transfer, signal captioning, and question answering. It achieves a 77.14% average linear-probing accuracy, a 5.93% relative improvement over strong baselines, and reaches 64.83% accuracy in sensor-based question answering. All code and datasets are publicly available at <https://github.com/yuc0805/SLIP>.

¹Dartmouth College. Correspondence to: Yuliang Chen <yuliang.chen.gr@dartmouth.edu>.

Preprint. March 13, 2026.

1. Introduction

Ubiquitous sensors continuously generate large volumes of multivariate time series data, motivating self-supervised pretraining as a way to learn transferable representations without costly annotations. Recent work shows that such pretraining can improve performance across diverse downstream tasks spanning health, activity recognition, and urban environment monitoring (Spathis et al., 2022; Thapa et al., 2026; Li et al., 2025). Alongside these efforts, general-purpose time series foundation models trained on heterogeneous sensor corpora using reconstruction or regression objectives, such as Chronos-2 (Ansari et al., 2025), have emerged. While effective for forecasting, these models primarily capture local temporal continuation and often fail to encode the semantic structure required for downstream classification and reasoning tasks (Figure 1). By contrast, sensor-specific pretraining frameworks tailored to individual modalities (*e.g.*, ECG or PPG) achieve strong in-domain performance (Pillai et al., 2024; Saha et al., 2025; McKeen et al., 2025), but typically struggle to generalize across different types of sensors or tasks.

Recently, large language models (LLMs) have showcased strong semantic abstraction and generalization, particularly in zero-shot and few-shot settings. Consequently, recent work explores aligning LLMs with time-series and sensor representations to overcome the limitations of reconstruction-based or sensor-specific pretraining. For instance, HealthLLM (Kim et al., 2024) reformulates sensor signals as text to directly leverage pretrained LLMs; however, this often leads to substantial semantic and temporal information loss. To better preserve signal structure, methods such as Time-LLM (Jin et al., 2023) and ChatTS (Xie et al., 2024) map the time series into the LLM embedding space via projection layers and rely on the language model for contextual inference. A complementary line of work uses contrastive cross-modal architectures to directly align sensor and text modalities, enabling zero-shot retrieval alongside generation (Ndir et al., 2025; Zhang et al., 2025). Despite progress in sensor–language alignment, most methods tie the sensor encoder to a fixed input specification, such as a predefined channel set or temporal resolution, limiting transfer when sensor configurations change and necessitating retraining. For instance, SensorLM (Zhang et al., 2025)

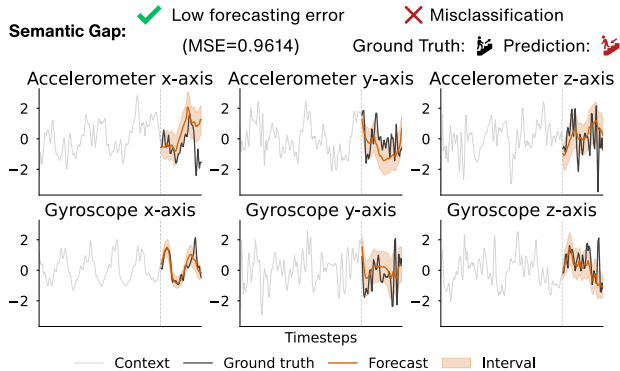


Figure 1. Illustrated example of the forecasting-classification gap. Chronos-2 achieves accurate forecasting on UCI-HAR with low error (MSE = 0.96), yet its learned representations lead to incorrect activity classification (walking downstairs vs. upstairs). This example illustrates that SSL-based models optimized for forecasting do not necessarily learn semantic representations that support downstream classification and understanding.

is limited by its fixed 26-channel, 1440-minute pretraining, which hinders transfer to varying sensor layouts or temporal resolutions.

To address these challenges, we propose SLIP, a unified language-informed sensor encoder trained via contrastive alignment to support heterogeneous sensor configurations, including multiple modalities and various temporal resolutions, and enable generalization to downstream tasks across different sensor domains. SLIP departs from prior sensor-language models in three key ways. First, to ensure broad cross-domain coverage, we pretrain on a mixture of heterogeneous time-series datasets, moving beyond the single-device specialization common in prior work. Second, to handle structural variations in sensor inputs, we introduce *FlexMLP*, a weight-sharing patch embedding mechanism that allows the model to dynamically adapt to different temporal resolutions without requiring retraining. Finally, instead of pretraining a decoder-only model (Xie et al., 2024; Langer et al., 2025), SLIP repurposes a pretrained decoder-only language model into an encoder-decoder architecture by decoupling it into a text encoder and a generative decoder, and extending the decoder with cross-attention to condition generation on sensor representations to enable unified sensor language understanding and open vocabulary generation across diverse downstream tasks. We summarize these capability differences against forecasting foundation models and recent sensor language models in Table 1.

Toward sensor-language models that capture semantic structure across heterogeneous sensor configurations, our contributions are as follows: (1) **Unified language-aligned sensor modeling:** We introduce SLIP, a unified sensor model that aligns heterogeneous multivariate time series with language, enabling a broad range of sensor-language tasks. Using the proposed *FlexMLP*, a lightweight mech-

Table 1. Capability comparison of sensor text modeling approaches. We compare prior studies and SLIP across key capabilities, including temporal resolution adaptive sensing to handle different input sequence length and frequency, sensor-text retrieval to capture semantic meaning, sensor question answering (QA), and open source availability.

Study	Resolution Adaptive	Retrieval	QA	Open Source
Chronos (Ansari et al., 2024)	✗	✗	✗	✓
Chronos2 (Ansari et al., 2025)	✗	✗	✗	✓
Sundial (Liu et al., 2025)	✗	✗	✗	✓
SensorLM (Zhang et al., 2025)	✗	✓	✗	✗
Normwear (Luo et al., 2025)	✗	✓	✗	✓
ChatTS (Xie et al., 2024)	✗	✗	✓	✓
OpenTSLM (Langer et al., 2025)	✗	✗	✓	✓
SLIP (ours)	✓	✓	✓	✓

anism for handling diverse sensor inputs, and repurposing decoder-only text models for efficient training, SLIP improves efficiency while maintaining cross-domain adaptability. (2) **Comprehensive multi-domain evaluation:** We evaluate SLIP across 11 diverse sensor datasets spanning human activity recognition, clinical diagnosis, stress prediction, and urban sensing, demonstrating consistent improvements in linear-probing classification, with an average accuracy of 77.15% compared to the strongest baseline, Normwear, at 72.82%, and competitive performance relative to supervised baselines at 76.2%. (3) **Open-vocabulary reasoning and generation:** We show that SLIP adapts effectively to open-vocabulary downstream tasks, with SLIP_{SFT} achieving strong sensor question answering performance of 64.83% average across four benchmarks and generating high-fidelity sensor captions with a BERTScore of 0.887. (4) **Curated sensor-language pretraining data:** To support sensor-language alignment at scale, we curate a dataset of 600K sensor-caption pairs spanning over 1 billion time points across diverse sensing domains including health, environment, Internet of Things, energy, and transportation, which we will release upon acceptance together with model weights and code to support further research.

2. Related Work

Time series and sensor foundation models. Sensor waveform signals derived from wearable devices are inherently time series data. Early efforts to learn transferable representations of such signals typically rely on large-scale self-supervised pretraining, using objectives such as masked reconstruction (Dong et al., 2023; Nie et al., 2023) or contrastive learning (Zhang et al., 2022). More recently, general-purpose time-series foundation models, including Chronos, Chronos-2, and Moment, have been trained on diverse domains such as electricity, finance, and climate (Ansari et al., 2024; 2025; Woo et al., 2024; Goswami et al., 2024). While these models demonstrate strong performance on forecast-

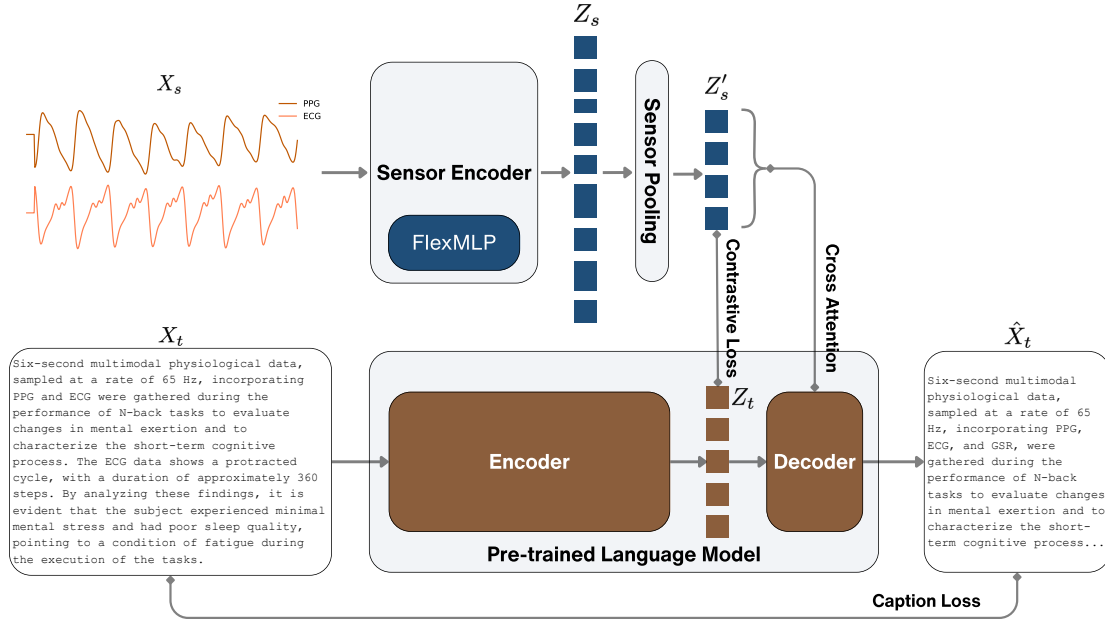


Figure 2. Sensor-Language Informed Pretraining (SLIP) Architecture.

ing tasks, they are primarily optimized for generative objectives and often generalize poorly to classification problems, which dominate many real-world sensor-based applications. To address this limitation, recent work has explored domain-specific sensor foundation models pretrained on large-scale physiological and behavioral datasets (Abbaspourazad et al., 2023; Narayanswamy et al., 2024; Xu et al., 2025; Qiu et al., 2025). For example, PPG-specific (Pillai et al., 2024; Saha et al., 2025) or ECG-specific models have shown improved accuracy, robustness, and generalizability within their target domains. However, despite their strong performance on narrow tasks, these domain-specific sensor models lack versatility and generalizability to diverse sensor data and tasks.

LLMs for time series and sensor models. Recently, integrating language models into time-series and sensor representation learning has emerged as a promising direction (Zhang et al., 2025; Langer et al., 2025; Pillai et al., 2025; Luo et al., 2025; Jin et al., 2023; Hu et al., 2025). Approaches such as Time-LLM or FSCA (Jin et al., 2023; Hu et al., 2025) reprogram time-series inputs into the embedding space of pretrained large language models, enabling LLMs to capture high-level semantic structure in temporal data. In parallel, cross-modal approaches through contrastive alignment, such as CoCa (Yu et al., 2022) explicitly align sensor signals with natural language descriptions, leveraging language as a rich source of semantic supervision. For example, SensorLM (Zhang et al., 2025) aligns FitBit wearable sensor streams with natural language via a hierarchical captioning pipeline and large-scale sensor–text pretraining, enabling improved zero- and few-shot recognition,

cross-modal retrieval, and semantic grounding in human activity and health tasks. Similarly, Hu et al. (2025) propose a context-alignment paradigm that structures time-series data and language into graph representations to activate and enhance pretrained large language models for time-series tasks, showing strong few- and zero-shot forecast performance. However, these approaches largely focus on specific sensor domains with fixed input lengths, which limits their ability to generalize across diverse sensors and tasks.

In contrast, we propose a unified language-informed sensor pretraining framework that supports heterogeneous sensor domains and variable temporal resolutions, enabling strong generalization across tasks ranging from classification to question answering.

3. Methodology

SLIP is a conceptual extension of CoCa for learning transferable language-aligned sensor representations for sensor-language applications that require both strong sensor understanding and contextual reasoning. SLIP is trained with paired $\langle X_s, X_t \rangle$ where X_s denotes the **sensor input** (a multivariate time series) and X_t is the **textual description** of X_s . SLIP comprises four components (Figure 2):

Sensor Encoder ($X_s \mapsto Z_s$) compresses high-volume sensor inputs to compact sensor embeddings Z_s – a sequence of continuous vectors analogous to “tokens”. Our sensor encoder uses a Transformer backbone with 120M parameters (Vaswani et al., 2023; Nie et al., 2023). We incorporate several design choices from Sundial (Liu et al., 2025), including

Pre-LN and FlashAttention for training stability and efficiency respectively. Because sampling frequencies such as minutely, hourly, or daily strongly affects which patterns are present in a series, we also make the patch-embedding frequency aware. Moirai (Woo et al., 2024) partially addresses this by assigning a fixed linear projection per frequency band via predefined patch sizes, and shows that resolution specific patch sizes can improve both accuracy and efficiency. Following this direction, we introduce *FlexMLP*, an elegant architectural modification that enables variable patch sizes with zero additional parameters or computational overhead. It combines the idea from FlexiViT (Beyer et al., 2023), which reuses one patch-embedding across patch sizes by resizing the patch-embedding weights, and the Chronos2 MLP patch-embedder (Ansari et al., 2025), namely encoding inputs with time indices and a timestep mask explicitly to represent missing values. Concretely, this embedder projects patchified sequences with arbitrary patch sizes into the same hidden dimension (i.e., 768), and sequences with fewer patches are padded to a uniform number of patches for batch processing. This design overcomes the fundamental challenge of conventional encoders by moving beyond fixed patch sizes, thereby providing dynamic granularity that adapts to varying sampling rates and sensor windows without retraining. Algorithm 1 summarizes a general recipe to flexify an existing MLP patch-embedder. This flexibility lets us increase the patch size for long sequences, which reduces the token count and makes it feasible to run full self-attention over all tokens from the entire multivariate time series. Concretely, we concatenate patch tokens from every sensor into a single 1D sequence and apply standard self-attention so that each token can attend to any other token, enabling global cross sensor and long range temporal interactions. To preserve the underlying 2D structure after concatenation, we use 2D RoPE (Su et al., 2023). In § 5.2, we also compare against the more efficient group attention from Chronos2 (Ansari et al., 2025), but find that self-attention coupled with 2D-RoPE performs better for question answering tasks empirically.

Sensor Pooler. ($Z_s \mapsto Z'_s$) is an attention pooling layer to compress the variable-length sensor sequence into a fixed-size representation Z'_s , abstracting away task-irrelevant noise. We follow CoCa and use a single multi-head cross-attention pooling layer with learnable query tokens. The sensor encoder output tokens are used as keys and values, and the queries produce a fixed-length set of pooled tokens. The number of pooled tokens is set by the number of queries. We heuristically use 65 query tokens in total: one classification token that summarizes the global sensor representation for contrastive learning, followed by 64 caption query tokens that condition the multimodal decoder, following BLIP-2 with an 8 times temporal compression (Li et al., 2023).

Algorithm 1 Minimal FlexMLP pseudo-implementation.

```

1
2 class FlexMLP(nn.Module):
3     def __call__(self, x, mask, time_index
4         , base_patch=16):
5         '''
6         x, mask, time_index: (B, L)
7         hidden_dim = 768
8         mlp_dim = 3072
9         '''
10        x_p = patchify(x, patch_size)
11        m_p = patchify(mask, patch_size)
12        t_p = patchify(t, patch_size) # (B, num_patches,
13            patch_size)
14        z_p = concat([x_p, m_p, t_p], axis=-1) # (B,
15            num_patches, patch_size*3)
16
17        # Shared MLP weights trained at base_patch:
18        w = self.param("w_mlp", (mlp_dim, base_patch*3))
19        b = self.param("b_mlp", (mlp_dim,))
20        w_res = self.param("w_res", (hidden_dim,
21            base_patch*3))
22        b_res = self.param("b_res", (hidden_dim,))
23
24        # Flex trick: resize weights to match current
25        patch size:
26        w_p = resize(w, (mlp_dim, patch_size*3))
27        w_res_p = resize(w_res, (hidden, patch_size*3))
28        h = linear(z_p, w_p, b)
29        r = linear(z_p, w_res_p, b_res)
30
31        # Fixed output projection:
32        w_out = self.param("w_out", (hidden_dim, mlp_dim
33            ))
34        b_out = self.param("b_out", (hidden_dim,))
35        h = linear(h, w_out, b_out)
36
37        return MLP(h) + r

```

Notes: FlexMLP pseudo implementation. The module supports variable patch sizes by resizing MLP weights learned at $base_patch = 16$ to the runtime $patch_size$, allowing a single encoder to process different temporal resolutions without retraining. Changes to existing code are highlighted with a violet background.

Text Encoder-Decoder. Text Encoder ($X_t \mapsto Z_t$) processes the textual description using a unimodal transformer to produce latent text representations Z_t , and **Multimodal Decoder** ($(Z'_s, Z_t) \mapsto \hat{X}_t$) fuses the unimodal text features Z_t with the pooled sensor embeddings Z'_s via cross-attention, where both representations are aligned before fusion, to predict target textual description \hat{X}_t . The text encoder is initialized from the first 12 layers of Gemma-3-270M (Team et al., 2025) so its parameter budget is in the same range as the text encoders commonly used in CoCa and CLIP, while the multimodal decoder is initialized from the final 6 layers of the same model. To condition text generation on sensor representations, we insert a cross-attention layer into each of the final six unimodal layers, transforming them into a multimodal decoder in which text tokens can attend to sensor encoder outputs during autoregressive decoding. For efficiency and training stability, we only unfreeze the last 4 layers of the unimodal text encoder, resulting in 220M total parameters with 67M trainable parameters. We analyze the effect of freezing the entire text encoder in Section 5.2. We also reuse the Gemma-3-270M tokenizer and token embedding, and cap the input at 512 query tokens, padding

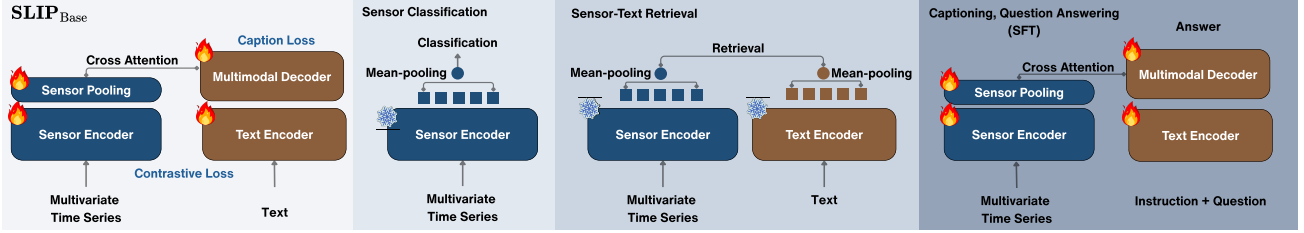


Figure 3. Overview of the pretrained SLIP that can be used for downstream tasks, including sensor classification and sensor text retrieval using the frozen encoders, and supports sensor captioning and question answering after supervised finetuning (SFT) to equip it with instruction following ability.

shorter queries with [PAD]. After adding cross-attention, we train the decoder with full parameters (43M trainable parameters). In summary, this branch closely follows the Gemma-3-270M architecture, introducing only 9M additional parameters via cross-attention.

Training Objectives. SLIP is optimized with two objectives jointly: (1) a contrastive loss that aligns global sensor embeddings with global text embeddings, encouraging matched sensor caption pairs to score higher than mismatched pairs in the batch, following the CLIP style objective (Radford et al., 2021); and (2) a captioning loss that trains a multimodal decoder to autoregressively generate the caption conditioned on the sensor embedding, providing a denser supervision signal that captures finer grained temporal structure, following CoCa (Yu et al., 2022). We optimized the two losses with equal weight throughout training such that

$$\mathcal{L}_{\text{Total}} = \mathcal{L}_{\text{contrastive}} + \mathcal{L}_{\text{caption}} \quad (1)$$

$$\mathcal{L}_{\text{Con}} = -\frac{1}{N} \left(\underbrace{\sum_i \log \frac{\exp(x_i^\top y_i / \sigma)}{\sum_{j=1}^N \exp(x_i^\top y_j / \sigma)}}_{\text{sensor-to-text}} + \underbrace{\sum_i \log \frac{\exp(y_i^\top x_i / \sigma)}{\sum_{j=1}^N \exp(y_i^\top x_j / \sigma)}}_{\text{text-to-sensor}} \right) \quad (2)$$

$$\mathcal{L}_{\text{Cap}} = - \sum_{t=1}^T \log P_\theta(y_t | y_{<t}, x). \quad (3)$$

Dataset. Pretraining SLIP requires large-scale paired time-series and text data, which is far less available than in vision–language settings. We start from community-released time series corpora (Liu et al., 2024; Luo et al., 2025) that provide diverse signals without aligned text, and we generate multi-level captions at statistical, structural, and semantic levels following the SensorLM recipe. To further increase pattern diversity, we augment this corpus with synthetic time series–text pairs from ChatTS (Xie et al., 2024). The resulting pretraining set contains over 600K samples and approximately one billion time points spanning energy, environment, health, IoT, nature, transportation, and web domains, with sampling rates ranging from seconds to months and varied sequence lengths. To reduce template repetition, we prompt Qwen2-7B-IT (Yang et al., 2024) to generate three paraphrases per caption and randomly sample one

during training. As in ChatTS, we sample multivariate and univariate examples with a 2:1 ratio. Corpus statistics are summarized in Table 7.

4. Experiments

Figure 3 summarizes the downstream uses of SLIP. We first describe the evaluation datasets (§ 4.1), followed by experimental setups for sensor classification (§ 4.2), zero-shot classification (§ 4.3), and supervised finetuning (§ 4.4).

4.1. Evaluation Datasets

We evaluate sensor-only perception tasks and zero-shot sensor–text retrieval across 11 datasets spanning four task domains: activity recognition (WISDM, UCIHAR), clinical diagnosis (Stroke, Diabetes, Hypertension, Sleep Stage, Heart Condition), stress prediction (WESAD, StudentLife), and urban sensing (Obstacles, BeijingAQI). We treat urban sensing as a more challenging setting, as our pretraining corpus contains limited in-domain data for this category. Table 8 summarizes the sensor modalities and label taxonomies for each dataset. We use the QA datasets with the same train-val-test split that OpenTSLM provided for free-form question-answering (HAR-CoT, Sleep-CoT, ECG-QA-CoT); and we reformat TSQA with a multiple-choice question (MCQ) protocol (Zellers et al., 2018) to evaluate basic sensor understanding and instruction following. For sensor captioning, we use the same M4 dataset as OpenTSLM.

4.2. Sensor Classification

We evaluate SLIP_{Base} on a diverse suite of 11 classification benchmarks spanning multiple domains, including activity recognition, clinical diagnosis, stress prediction, and urban sensing.

For each dataset, we compute the sensor representation by mean pooling all patch token embeddings from the pre-trained sensor encoder, and train a linear classifier on top of these resulting frozen features. As demonstrated in prior multimodal representation learning work (Radford et al., 2021), linear evaluation provides a more direct assessment

Table 2. Evaluation of the SLIP_{Base} on 11 downstream sensor tasks across 4 domains compared against multiple baselines with linear-probing. We report the top-1 accuracy on the test set. Best performance in each dataset are **highlighted**.

Model	# Parameters	# Time Points	Activity Recognition			Clinical Diagnosis					Stress Prediction			Urban Sensing			
			Average	WISDM	UCIHAR	Average	Stroke	Diabetes	Hypertension	Sleep Stag.	Heart Cond.	Average	WESAD	Studentlife	Average	Obstacles	Beijing AQI
Statistical ML	-	-	78.34	72.43	84.24	70.87	90.15	82.22	37.88	78.95	65.15	55.70	62.78	48.62	74.97	81.33	68.6
SimMTM	0.5M	1.72M	58.35	44.93	71.75	62.55	89.39	82.22	38.64	46.34	56.18	62.20	75.78	48.62	71.85	76.47	67.23
TF-C	12M	1.72M	59.6	55.39	63.81	63.66	90.91	82.96	39.39	46.97	58.06	39.58	56.95	42.20	47.98	49.87	46.08
Sundial _{Base}	128M	1032B	70.07	81.25	58.89	69.04	90.91	82.22	42.42	68.69	60.97	49.29	56.50	51.38	53.94	68.80	66.55
Chronos _{Base}	200M	12.8B	81.07	80.30	81.84	70.85	81.06	77.78	46.97	76.68	71.76	57.50	66.37	48.62	77.02	75.19	78.84
Chronos2	120M	242.8B	77.74	75.02	80.45	71.89	90.91	77.04	47.73	82.48	61.27	60.40	73.09	47.71	65.67	81.84	49.49
Normwear	136M	0.31B	74.98	70.77	79.19	73.00	90.91	82.22	40.15	82.57	69.15	63.99	80.27	47.71	79.06	83.38	74.74
ChatTS	8B	0.23B	62.57	75.59	49.55	71.88	90.91	82.22	38.63	80.53	67.09	63.79	78.03	49.54	68.23	76.73	59.73
SLIP_{Base}	120M	1.7B	84.31	82.36	86.25	75.59	91.67	84.44	50.00	82.04	70.79	68.55	82.96	54.13	81.96	86.45	77.47
<i>PatchTST (Supervised Learning)</i>	<i>0.9M</i>	-	85.08	85.66	84.49	76.52	90.91	82.96	48.48	84.29	75.94	62.20	75.78	48.62	80.51	84.91	76.11

of representation quality by limiting the model’s capacity to compensate for weak features during downstream adaptation. This evaluation choice aligns with our goal of developing a task- and dataset-agnostic pretraining approach that yields strong performance without reliance on task-specific finetuning. In terms of **baselines**, we compare SLIP against several categories of prior work. These include self-supervised learning methods such as SimMTM and TF-C (Dong et al., 2023; Zhang et al., 2022), as well as general-purpose time-series foundation models including Sundial, Chronos, and Chronos-2. We additionally consider models that incorporate natural language supervision, such as NormWear and ChatTS (Luo et al., 2025; Xie et al., 2024). As an upper bound, we include PatchTST (Nie et al., 2023) trained in a fully supervised setting.

4.3. Zero-shot Understanding

Sensor-Text Retrieval. Following CLIP (Radford et al., 2021), we evaluate representation alignment with a sensor text-retrieval protocol: each sensor sample is represented by mean pooling the token outputs from the frozen sensor encoder, each class prompt is represented by a text prototype formed by mean-pooling over the language encoder token embeddings, and labels are predicted by nearest neighbor matching under cosine similarity in the shared embedding space. Because most time-series foundation models are trained solely on numerical signals and never exposed to text, they are not applicable in this task. Under this protocol, we only compare SLIP_{Base} against NormWear, which also incorporates language supervision.

Additional Baselines. To further contextualize performance, we evaluate open-weight language models (Gemma3-270M-IT, Gemma3-4B-IT) and the recent time-series language model ChatTS using unified multiple-choice question (MCQ) prompting (Zellers et al., 2018) (examples in Figs. 9, 10). Unlike ChatTS, which directly processes

time-series inputs, language-only and vision-language baselines require explicit input adaptations. We consider two settings: (1) Text prompting, where numerical time series are serialized as text and provided to Gemma3 following prior work (Liu et al., 2023); and (2) Image prompting, where time series are converted into plots (Wimmer & Rekabsaz, 2023) and supplied as visual inputs to Gemma3-4B-IT.¹ All models are evaluated using the same MCQ template (examples in Figures 5,6,7,8). with Top-1 accuracy indicating correct option selection. We do not prompt SLIP_{Base} in this experiment, as it lacks instruction-following capability; this is instead evaluated via supervised finetuning in § 4.4.

4.4. Supervised Finetuning

Question Answering. Sensor QA is an emerging paradigm that enables open-ended natural language queries grounded in fine-grained temporal signals, offering greater flexibility than fixed-label prediction. We introduce SLIP_{SFT}, which applies supervised finetuning to SLIP_{Base} using the captioning loss only. We benchmark against OpenTSLM (Langer et al., 2025) using both soft prompting and Flamingo open-weight variants with a Gemma3-270M backbone for architectural parity, evaluating all models on identical datasets and splits. In contrast to OpenTSLM’s multi-stage curriculum training across TSQA, HAR-CoT, Sleep-CoT, and ECG-QA-CoT for over 40 epochs, SLIP_{SFT} adopts a minimal finetuning protocol, finetuning SLIP_{Base} independently on each dataset for four epochs (ten for Sleep-CoT). This setting isolates the contribution of pretrained sensor-language representations rather than extensive task-specific optimization.

Sensor Captioning. Pretrained with an encoder-decoder objective, SLIP_{Base} supports sensor captioning without architectural changes and generates natural language descrip-

¹Gemma3-270M-IT does not support visual inputs.

Table 3. **Zero shot evaluation on 11 downstream tasks.** We compare the proposed methods with Normwear under the same sensor text retrieval based zero shot setting, and also include additional open weight LLM and VLM baselines evaluated using a multiple choice question protocol. All results report top one accuracy (R@1) on the test set.

Inference Type	Model	# Avg. tokens	Activity Classification			Average	Clinical Diagnosis					Average	Stress Prediction		Urban Sensing		
			Average	WISDM	UCHAR		Stroke	Diabetes	Hypertension	Sleep Stag.	Heart Cond.		WESAD	Studentlife	Average	Obstacles	Beijing AQI
MCQ	LLM-Text (gemma-3-270M-it)	37k	13.31	5.18	21.44	29.54	9.09	17.78	38.64	26.93	55.27	-	OOM	OOM	35.15	20.46	49.83
	LLM-Text (gemma-3-4b-it)	37k	11.10	6.05	16.14	21.15	9.09	17.78	37.12	27.05	14.73	-	OOM	OOM	18.43	14.32	22.53
	VLM-Images (gemma-3-4b-it)	370	15.33	6.07	24.59	33.25	90.91	31.11	15.91	13.64	14.67	41.25	43.05	39.45	39.11	28.39	49.83
	ChatTS-8B	1k	15.58	8.32	22.83	29.10	9.91	29.63	38.64	13.79	53.52	25.56	30.94	20.18	36.43	23.02	49.83
Retrieval	Normwear (w/ Mstif)	9k	8.45	3.91	12.99	52.52	89.39	82.22	36.36	39.09	15.52	29.86	16.59	43.12	13.35	24.30	2.39
	SLIP_{Base} (Gemma-3-270M)	300	17.54	7.45	27.62	49.11	86.40	74.07	34.85	34.83	15.39	49.11	56.95	41.28	27.08	29.92	24.23

Table 4. **Time series captioning results on the M4 caption test set.** All models use Gemma3-270M as the language backbone. We report both surface level and semantic evaluation metrics, where BLEU at four, METEOR, and ROUGE-L measure n-gram overlap, and SBERTSimilarity and BERTScore measure semantic similarity. Higher values indicate better performance for all metrics.

Model	BLEU@4	METEOR	ROUGE-L	SBERTSimilarity	BERTScore
OpenTSLM SP	0.0026	0.0456	0.0255	0.1551	0.7250
OpenTSLM Flamingo	0.1141	0.3210	0.2894	0.7990	0.8858
SLIP _{Base}	0.0116	0.2440	0.1409	0.6276	0.8338
SLIP _{SFT}	0.1130	0.3814	0.2569	0.8691	0.8870

tions conditioned on multivariate time series inputs. To evaluate adaptation to a new caption style, we finetune SLIP_{Base} for four epochs on the M4 training split and evaluate SLIP_{SFT} on the M4 test split. We compare against OpenTSLM Flamingo and OpenTSLM soft prompting, reporting BLEU@4 (Papineni et al., 2002), METEOR (Banerjee & Lavie, 2005), ROUGE-L (Lin, 2004), SBERTSimilarity (Reimers & Gurevych, 2019), and BERTScore (Zhang et al., 2020); all are higher is better.

5. Results & Discussion

5.1. Overall Performance

SLIP_{Base} achieves the strongest average linear-probe accuracy across 11 sensor classification datasets. From Table 2, SLIP_{Base} outperforms the strongest baseline, NormWear (77.14 vs. 72.82), and performs on par with the supervised PatchTST (76.2%). Per-dataset results show particularly strong performance on stress prediction tasks such as WESAD and StudentLife. Notably, despite being pretrained on substantially less urban sensing data (fewer than 50k samples) than forecasting-based models, SLIP_{Base} remains competitive. The complete 5 fold evaluation results and F1 scores are reported in Table 13 and Table 12.

SLIP_{Base} achieves the highest average zero-shot accuracy across 11 sensor classification tasks while requiring substantially less inference compute. Table 3 compares SLIP_{Base} with the baselines described in Section 4.3 under a

Table 5. **Performance on sensor QA task.** All models use the same Gemma-3-270M language backbone for a controlled comparison. TSQA is evaluated using a multiple choice question protocol, while HAR-CoT, Sleep-CoT, and ECG-QA-CoT use a free form generation protocol. All results report accuracy on the test set.

Model	TSQA	HAR-CoT	Sleep-CoT	ECG-QA-CoT
OpenTSLM-SP	11.96	0.55	5.91	1.11
OpenTSLM-Flamingo	25.46	63.43	68.49	35.50
SLIP_{SFT}	83.60	64.35	74.19	37.18

more challenging zero-shot setting. SLIP_{Base} outperforms many competing approaches while using orders of magnitude fewer tokens at inference time: on average, SLIP requires approximately 300 tokens per sample, whereas prompting-based LLM and VLM methods require around 37,000 tokens. SLIP_{Base} performs particularly well on stress prediction tasks, which benefit from higher-level behavioral and physiological patterns that map to interpretable states (e.g., phone usage). In contrast, it is relatively weaker on clinical diagnosis compared with NormWear, which is pretrained on matched high-frequency clinical signals and aligns sensor representations with ClinicalTinyLlama, providing stronger coverage of symptom-level details. Overall, SLIP_{Base} achieves the highest average zero-shot accuracy (39.42%) across 11 tasks, compared with 30.42% for NormWear. Interestingly, text-only approaches perform competitively on certain datasets (e.g., Heart Condition, Beijing Air Quality), likely because these tasks admit strong inductive rules that language models capture well (e.g., strong winds clearing urban smog).

SLIP_{Base} provides a strong initialization for sensor question answering with minimal finetuning. As shown in Table 5, SLIP_{SFT} outperforms OpenTSLM under both soft prompting and Flamingo-style training while using the same language backbone. These results indicate that SLIP’s sensor encoder yields more effective representations for downstream question answering, enabling improved adaptation under limited task-specific supervision.

SLIP_{Base} generates semantically aligned sensor captions

Table 6. **Ablation studies results.** The default setting adopted by SLIP is marked in blue. We calculate $\pm\delta$ within each group of ablations in comparison with the default setting.

	Sensor Perception (Accuracy)	Retrieval (Accuracy)	QA (Accuracy)
<i>(a) Training Objectives</i>			
SLIP pretraining	77.14	39.36	64.83
Caption-only	74.30 (-2.84)	25.12 (-14.24)	57.26 (-7.57)
Contrastive-only	74.77 (-2.37)	36.90 (-2.46)	48.03 (-9.98)
Random paired	62.15 (-14.99)	22.38 (-16.98)	35.08 (-29.75)
<i>(b) Sensor Encoder Parameter Size</i>			
SLIP _{small} (40M)	74.84 (-2.30)	26.71 (-12.65)	53.99 (-10.84)
<i>(c) Cross-Sensor Learning</i>			
Self-Attention w/ 2D RoPE	77.14	39.36	64.83
Group Attention	77.04 (-0.10)	39.21 (-0.15)	58.01 (-6.82)
<i>(d) FlexMLP</i>			
w/o FlexMLP (patch size = 16)	74.16 (-2.98)	34.79 (-4.42)	61.38 (-3.45)
<i>(e) Partial finetuning of text-encoder</i>			
Fine-tune 4-layer	77.14	39.36	64.83
Freeze	73.56 (-3.58)	35.68 (-3.68)	57.09 (-7.74)

without task-specific training. As shown in Table 4, SLIP_{Base} produces captions that preserve the main semantic content of the time series despite not being trained on any M4 examples, as reflected by strong SBERTSimilarity (0.6279) and BERTScore (0.8870). In contrast, lower n-gram overlap metrics such as BLEU@4, METEOR, and ROUGE-L indicate stylistic differences, since the M4 references follow a different writing style than the captions used during pretraining. After finetuning on the M4 training split, SLIP_{SFT} generates captions that more closely match the reference phrasing while maintaining linguistic diversity, and further improves semantic alignment at both the sentence and token levels. Notably, SLIP_{SFT} achieves n-gram-based scores comparable to OpenTSLM Flamingo, suggesting that many remaining discrepancies reflect paraphrasing rather than semantic errors.

5.2. Ablation Studies

We study key design choices in SLIP and report average top-1 classification accuracy, zero-shot classification accuracy (both over 11 datasets), and QA accuracy (over 4 datasets).

Training Objectives. We compare SLIP against single-objective variants in Table 5.2. Relative to a contrastive-only model, SLIP improves supervised classification (+2.37), zero-shot retrieval (+2.46), and yields a substantial gain in QA (+9.98), indicating that the captioning objective provides complementary semantic supervision. Additionally, SLIP substantially outperforms a caption-only model in retrieval (+14.24) and QA (+7.57), suggesting that while caption-only models can generate fluent text, their sensor embeddings remain weakly grounded in the input signals. Using metrics from Wang & Isola (2022), Figure 4 shows that the caption-only model suffers from poor sensor-text alignment and degraded sensor and text uniformity, consistent with representation collapse. More details about alignment and uniformity can be found in Appendix § F. We also include SLIP trained with intentionally misaligned sensor-text pairs as a simple sanity check against the aligned training setup.

Model Size. Using a smaller sensor encoder (40M) leads

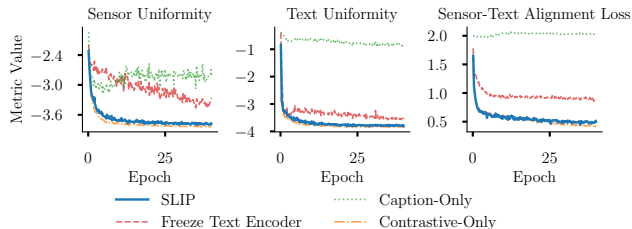


Figure 4. **Sensor-Language representation geometry Analysis.** **Sensor Uniformity (left)** and **Text Uniformity (middle)** quantify embedding dispersion on the unit hypersphere, while **Sensor-Text Alignment (right)** measures the mean distance between paired sensor and text embeddings. Lower values indicate better performance across all metrics.

to a substantial drop in retrieval (-12.65) and QA (-10.84), while sensor perception is less affected (-2.3). This suggests that although the smaller encoder preserves task-relevant features for linear separability, it fails to learn an embedding geometry that supports reliable cross-modal alignment. We attribute this to modality imbalance during training. That is, when the sensor branch becomes the bottleneck, optimization primarily adjusts the text branch and cross-modal projections, providing weaker gradients to shape sensor embeddings into a discriminative, well-aligned space. In practice, this imbalance could be mitigated through training heuristics such as staged unfreezing or branch-specific learning rates, which we leave to future work.

Cross-sensor Learning. Group attention shows negligible impact on sensor perception (-0.10) and zero-shot classification (-0.15), but leads to a sharp drop on the univariate TSQA dataset (-21.94), reducing average SFT performance by 6.82 (Table 16). We attribute this to multivariate-dominated pretraining encouraging cross-channel shortcuts under group attention; when evaluated on univariate TSQA, this signal is absent, weakening long-range evidence aggregation within a single channel. Brief supervised finetuning adjusts instruction following but does not correct this behavior. Overall, given comparable classification performance, group attention remains a practical option when memory constraints make full attention infeasible.

FlexMLP. Using a fixed patch size (e.g., 16) during pre-

training and evaluation degrades performance, particularly for zero-shot classification (-4.42), where no task-specific head aggregates information across patches. Because patch size determines temporal resolution, datasets with different sampling frequencies (*e.g.*, hourly vs. second-level) favor different patch granularities; we provide a simple rule of thumb for selecting patch size in Appendix §C.

Freezing Text Encoder. We evaluate a parameter-efficient variant of SLIP that freezes the text encoder and trains only the sensor encoder, projector, and multimodal decoder. As shown in Figure 4, this underperforms finetuned models: sensor features spread more slowly, plateau earlier, and exhibit weaker sensor–text alignment. Freezing the text encoder prevents mutual adaptation between modalities during contrastive learning, forcing the sensor encoder to match fixed text targets that may not reflect the underlying signals. As a result, sensor representations collapse toward a limited region of the feature space, leading to consistent degradation across downstream tasks.

6. Limitations

Some limitations of our work should be noted. First, to isolate the effects of sensor–text alignment, we fix the language model backbone; exploring alternative language models is left to future work. Second, compared to vision–language models that rely on short captions, SLIP conditions on longer free-form textual descriptions, increasing context length and computational cost during pretraining. Scalability could be improved through selective decoding or adaptive context compression. Finally, we do not analyze hallucination or output faithfulness, nor identify which temporal regions support specific generated claims; developing attribution and faithfulness analyses remains an important direction.

7. Conclusion

This paper introduces SLIP, a conceptual instantiation of Contrastive Captioners (CoCa) for sensor–language representation learning. Pretrained in a single stage on sensor–text pairs from diverse data sources, SLIP efficiently repurposes a decoder-only language model into a multimodal encoder–decoder model. SLIP_{Base} achieves state-of-the-art performance from a single checkpoint across diverse sensor application domains. We also show that SLIP_{SFT} can adapt to complex sensor question answering tasks with little finetuning. Our work helps address the lack of a unified, language-aligned sensor encoder that can encode diverse sensor inputs into language, and we hope it motivates new directions for large sensor–language foundation models.

Acknowledgments

The authors acknowledge support for this research from **Evergreen: A Generative AI and Behavioral Sensing Digital Ecosystem to Promote Student Wellness and Flourishing**. This work is made possible through philanthropic gifts to Dartmouth College dedicated to advancing AI-supported well-being and flourishing of college students.

References

- Abbaspourazad, S., Elachqar, O., Miller, A. C., Emrani, S., Nallasamy, U., and Shapiro, I. Large-scale training of foundation models for wearable biosignals. *arXiv preprint arXiv:2312.05409*, 2023.
- Ansari, A. F., Stella, L., Turkmen, C., Zhang, X., Mercado, P., Shen, H., Shchur, O., Rangapuram, S. S., Arango, S. P., Kapoor, S., Zschiegner, J., Maddix, D. C., Wang, H., Mahoney, M. W., Torkkola, K., Wilson, A. G., Bohlke-Schneider, M., and Wang, Y. Chronos: Learning the language of time series, 2024. URL <https://arxiv.org/abs/2403.07815>.
- Ansari, A. F., Shchur, O., Küken, J., Auer, A., Han, B., Mercado, P., Rangapuram, S. S., Shen, H., Stella, L., Zhang, X., Goswami, M., Kapoor, S., Maddix, D. C., Gueron, P., Hu, T., Yin, J., Erickson, N., Desai, P. M., Wang, H., Rangwala, H., Karypis, G., Wang, Y., and Bohlke-Schneider, M. Chronos-2: From univariate to universal forecasting, 2025. URL <https://arxiv.org/abs/2510.15821>.
- Banerjee, S. and Lavie, A. METEOR: An automatic metric for MT evaluation with improved correlation with human judgments. In Goldstein, J., Lavie, A., Lin, C.-Y., and Voss, C. (eds.), *Proceedings of the ACL Workshop on Intrinsic and Extrinsic Evaluation Measures for Machine Translation and/or Summarization*, pp. 65–72, Ann Arbor, Michigan, June 2005. Association for Computational Linguistics. URL <https://aclanthology.org/W05-0909/>.
- Beyer, L., Izmailov, P., Kolesnikov, A., Caron, M., Kornblith, S., Zhai, X., Minderer, M., Tschannen, M., Alabdulmohsin, I., and Pavetic, F. Flexivit: One model for all patch sizes, 2023. URL <https://arxiv.org/abs/2212.08013>.
- Chan, S., Yuan, H., Tong, C., Acquah, A., Schonfeldt, A., Gershuny, J., and Doherty, A. Capture-24: A large dataset of wrist-worn activity tracker data collected in the wild for human activity recognition, 2024. URL <https://arxiv.org/abs/2402.19229>.
- Chen, S. Beijing Multi-Site Air Quality. UCI

- Machine Learning Repository, 2017. DOI: <https://doi.org/10.24432/C5RK5G>.
- Demšar, J. Statistical comparisons of classifiers over multiple data sets. *J. Mach. Learn. Res.*, 7:1–30, December 2006. ISSN 1532-4435.
- Dong, J., Wu, H., Zhang, H., Zhang, L., Wang, J., and Long, M. Simmtm: A simple pre-training framework for masked time-series modeling, 2023. URL <https://arxiv.org/abs/2302.00861>.
- Goswami, M., Szafer, K., Choudhry, A., Cai, Y., Li, S., and Dubrawski, A. Moment: A family of open time-series foundation models. *arXiv preprint arXiv:2402.03885*, 2024.
- He, K., Chen, X., Xie, S., Li, Y., Dollár, P., and Girshick, R. Masked autoencoders are scalable vision learners, 2021. URL <https://arxiv.org/abs/2111.06377>.
- Hu, Y., Li, Q., Zhang, D., Yan, J., and Chen, Y. Context-alignment: Activating and enhancing llm capabilities in time series. *arXiv preprint arXiv:2501.03747*, 2025.
- Jin, M., Wang, S., Ma, L., Chu, Z., Zhang, J. Y., Shi, X., Chen, P.-Y., Liang, Y., Li, Y.-F., Pan, S., et al. Time-llm: Time series forecasting by reprogramming large language models. *arXiv preprint arXiv:2310.01728*, 2023.
- Kemp, B., Zwinderman, A., Tuk, B., Kamphuisen, H., and Oberye, J. Analysis of a sleep-dependent neuronal feedback loop: the slow-wave microcontinuity of the eeg. *IEEE Transactions on Biomedical Engineering*, 47(9): 1185–1194, 2000. doi: 10.1109/10.867928.
- Kim, Y., Xu, X., McDuff, D., Breazeal, C., and Park, H. W. Health-llm: Large language models for health prediction via wearable sensor data, 2024. URL <https://arxiv.org/abs/2401.06866>.
- Langer, P., Kaar, T., Rosenblattl, M., Xu, M. A., Chow, W., Maritsch, M., Verma, A., Han, B., Kim, D. S., Chubb, H., Ceresnak, S., Zahedivash, A., Sandhu, A. T. S., Rodriguez, F., McDuff, D., Fleisch, E., Aalami, O., Barata, F., and Schmiedmayer, P. Opentslm: Time-series language models for reasoning over multivariate medical text- and time-series data, 2025. URL <https://arxiv.org/abs/2510.02410>.
- Li, J., Li, D., Savarese, S., and Hoi, S. Blip-2: Bootstrapping language-image pre-training with frozen image encoders and large language models, 2023. URL <https://arxiv.org/abs/2301.12597>.
- Li, Z., Xia, L., Shi, L., Xu, Y., Yin, D., and Huang, C. Open spatio-temporal foundation models for traffic prediction. *ACM Transactions on Intelligent Systems and Technology*, October 2025. ISSN 2157-6912. doi: 10.1145/3773912. URL <http://dx.doi.org/10.1145/3773912>.
- Liang, Y., Chen, Z., Liu, G., Elgendi, M., Chen, Z., Ward, R., and Wang, Z. A new, short-recorded photoplethysmogram dataset for blood pressure monitoring in china. *Scientific Data*, 5:180020, 2018. doi: 10.1038/sdata.2018.20. URL <https://doi.org/10.1038/sdata.2018.20>.
- Lin, C.-Y. ROUGE: A package for automatic evaluation of summaries. In *Text Summarization Branches Out*, pp. 74–81, Barcelona, Spain, July 2004. Association for Computational Linguistics. URL <https://aclanthology.org/W04-1013/>.
- Liu, X., McDuff, D., Kovacs, G., Galatzer-Levy, I., Sunshine, J., Zhan, J., Poh, M.-Z., Liao, S., Achille, P. D., and Patel, S. Large language models are few-shot health learners, 2023. URL <https://arxiv.org/abs/2305.15525>.
- Liu, Y., Zhang, H., Li, C., Huang, X., Wang, J., and Long, M. Timer: Generative pre-trained transformers are large time series models, 2024. URL <https://arxiv.org/abs/2402.02368>.
- Liu, Y., Qin, G., Shi, Z., Chen, Z., Yang, C., Huang, X., Wang, J., and Long, M. Sundial: A family of highly capable time series foundation models, 2025. URL <https://arxiv.org/abs/2502.00816>.
- Loshchilov, I. and Hutter, F. Decoupled weight decay regularization, 2019. URL <https://arxiv.org/abs/1711.05101>.
- Luo, Y., Chen, Y., Salekin, A., and Rahman, T. Toward foundation model for multivariate wearable sensing of physiological signals, 2025. URL <https://arxiv.org/abs/2412.09758>.
- McKeen, K., Masood, S., Toma, A., Rubin, B., and Wang, B. Ecg-fm: An open electrocardiogram foundation model. *JAMIA open*, 8(5):ooaf122, 2025.
- Narayanswamy, G., Liu, X., Ayush, K., Yang, Y., Xu, X., Liao, S., Garrison, J., Taylor, S., Sunshine, J., Liu, Y., et al. Scaling wearable foundation models. *arXiv preprint arXiv:2410.13638*, 2024.
- Ndir, T. C., Schirrmeyer, R. T., and Ball, T. Eeg-clip : Learning eeg representations from natural language descriptions, 2025. URL <https://arxiv.org/abs/2503.16531>.
- Nie, Y., Nguyen, N. H., Sinthong, P., and Kalagnanam, J. A time series is worth 64 words: Long-term forecasting with transformers, 2023. URL <https://arxiv.org/abs/2211.14730>.

- Papineni, K., Roukos, S., Ward, T., and Zhu, W.-J. Bleu: a method for automatic evaluation of machine translation. In Isabelle, P., Charniak, E., and Lin, D. (eds.), *Proceedings of the 40th Annual Meeting of the Association for Computational Linguistics*, pp. 311–318, Philadelphia, Pennsylvania, USA, July 2002. Association for Computational Linguistics. doi: 10.3115/1073083.1073135. URL <https://aclanthology.org/P02-1040/>.
- Pillai, A., Spathis, D., Kawsar, F., and Malekzadeh, M. Pagei: Open foundation models for optical physiological signals. *arXiv preprint arXiv:2410.20542*, 2024.
- Pillai, A., Spathis, D., Nepal, S., Collins, A. C., Mackin, D. M., Heinz, M. V., Griffin, T. Z., Jacobson, N. C., and Campbell, A. Beyond prompting: Time2lang-bridging time-series foundation models and large language models for health sensing. In *Conference on Health, Inference, and Learning*, pp. 268–288. PMLR, 2025.
- Qiu, M., Weng, C., Fan, M., and Wu, K. Towards customizable foundation models for human activity recognition with wearable devices. *Proceedings of the ACM on Interactive, Mobile, Wearable and Ubiquitous Technologies*, 9(3):1–29, 2025.
- Radford, A., Kim, J. W., Hallacy, C., Ramesh, A., Goh, G., Agarwal, S., Sastry, G., Askell, A., Mishkin, P., Clark, J., Krueger, G., and Sutskever, I. Learning transferable visual models from natural language supervision, 2021. URL <https://arxiv.org/abs/2103.00020>.
- Reimers, N. and Gurevych, I. Sentence-bert: Sentence embeddings using siamese bert-networks, 2019. URL <https://arxiv.org/abs/1908.10084>.
- Reyes-Ortiz, J., Anguita, D., Ghio, A., Oneto, L., and Parra, X. Human Activity Recognition Using Smartphones. UCI Machine Learning Repository, 2013. DOI: <https://doi.org/10.24432/C54S4K>.
- Saha, M., Xu, M. A., Mao, W., Neupane, S., Rehg, J. M., and Kumar, S. Pulse-ppg: An open-source field-trained ppg foundation model for wearable applications across lab and field settings. *Proceedings of the ACM on Interactive, Mobile, Wearable and Ubiquitous Technologies*, 9(3):1–35, 2025.
- Schmidt, P., Reiss, A., Dürichen, R., Marberger, C., and Van Laerhoven, K. Introducing wesad, a multimodal dataset for wearable stress and affect detection. In *Proceedings of the 20th ACM International Conference on Multimodal Interaction (ICMI '18)*, pp. 400–408, New York, NY, USA, 2018. Association for Computing Machinery. doi: 10.1145/3242969.3242985.
- Souza, V. M. A. Asphalt pavement classification using smartphone accelerometer and complexity invariant distance. *Engineering Applications of Artificial Intelligence*, 74:198–211, 2018. ISSN 0952-1976. doi: 10.1016/j.engappai.2018.06.003. URL <https://www.sciencedirect.com/science/article/pii/S0952197618301349>.
- Spathis, D., Perez-Pozuelo, I., Gonzales, T. I., Wu, Y., Brage, S., Wareham, N., and Mascolo, C. Longitudinal cardio-respiratory fitness prediction through wearables in free-living environments. *NPJ Digital Medicine*, 5(1):176, 2022.
- Su, J., Lu, Y., Pan, S., Murtadha, A., Wen, B., and Liu, Y. Roformer: Enhanced transformer with rotary position embedding, 2023. URL <https://arxiv.org/abs/2104.09864>.
- Team, G., Kamath, A., Ferret, J., Pathak, S., Vieillard, N., Merhej, R., Perrin, S., Matejovicova, T., Ramé, A., Rivière, M., Rouillard, L., Mesnard, T., Cideron, G., bastien Grill, J., Ramos, S., Yvinec, E., Casbon, M., Pot, E., Penchev, I., Liu, G., Visin, F., Kenealy, K., Beyer, L., Zhai, X., Tsitsulin, A., Busa-Fekete, R., Feng, A., Sachdeva, N., Coleman, B., Gao, Y., Mustafa, B., Barr, I., Parisotto, E., Tian, D., Eyal, M., Cherry, C., Peter, J.-T., Sinopalnikov, D., Bhupatiraju, S., Agarwal, R., Kazemi, M., Malkin, D., Kumar, R., Vilar, D., Brusilovsky, I., Luo, J., Steiner, A., Friesen, A., Sharma, A., Sharma, A., Gilady, A. M., Goedeckemeyer, A., Saade, A., Feng, A., Kolesnikov, A., Bendebury, A., Abdagic, A., Vadi, A., György, A., Pinto, A. S., Das, A., Bapna, A., Miech, A., Yang, A., Paterson, A., Shenoy, A., Chakrabarti, A., Piot, B., Wu, B., Shahriari, B., Petrini, B., Chen, C., Lan, C. L., Choquette-Choo, C. A., Carey, C., Brick, C., Deutsch, D., Eisenbud, D., Cattle, D., Cheng, D., Paparas, D., Sreepathihalli, D. S., Reid, D., Tran, D., Zelle, D., Noland, E., Huizenga, E., Kharitonov, E., Liu, F., Amirkhanyan, G., Cameron, G., Hashemi, H., Klimczak-Plucińska, H., Singh, H., Mehta, H., Lehri, H. T., Hazimeh, H., Ballantyne, I., Szpektor, I., Nardini, I., Pouget-Abadie, J., Chan, J., Stanton, J., Wieting, J., Lai, J., Orbay, J., Fernandez, J., Newlan, J., yeong Ji, J., Singh, J., Black, K., Yu, K., Hui, K., Vodrahalli, K., Greff, K., Qiu, L., Valentine, M., Coelho, M., Ritter, M., Hoffman, M., Watson, M., Chaturvedi, M., Moynihan, M., Ma, M., Babar, N., Noy, N., Byrd, N., Roy, N., Momchev, N., Chauhan, N., Sachdeva, N., Bunyan, O., Botarda, P., Caron, P., Rubenstein, P. K., Culliton, P., Schmid, P., Sessa, P. G., Xu, P., Stanczyk, P., Tafti, P., Shivanna, R., Wu, R., Pan, R., Rokni, R., Willoughby, R., Vallu, R., Mullins, R., Jerome, S., Smoot, S., Girgin, S., Iqbal, S., Reddy, S., Sheth, S., Pöder, S., Bhatnagar, S., Panyam, S. R., Eiger, S., Zhang, S., Liu, T.,

- Yacovone, T., Liechty, T., Kalra, U., Evci, U., Misra, V., Roseberry, V., Feinberg, V., Kolesnikov, V., Han, W., Kwon, W., Chen, X., Chow, Y., Zhu, Y., Wei, Z., Egyed, Z., Cotruta, V., Giang, M., Kirk, P., Rao, A., Black, K., Babar, N., Lo, J., Moreira, E., Martins, L. G., Sanseviero, O., Gonzalez, L., Gleicher, Z., Warkentin, T., Mirrokni, V., Senter, E., Collins, E., Barral, J., Ghahramani, Z., Hadsell, R., Matias, Y., Sculley, D., Petrov, S., Fiedel, N., Shazeer, N., Vinyals, O., Dean, J., Hassabis, D., Kavukcuoglu, K., Farabet, C., Buchatskaya, E., Alayrac, J.-B., Anil, R., Dmitry, Lepikhin, Borgeaud, S., Bachem, O., Joulin, A., Andreev, A., Hardin, C., Dadashi, R., and Hussenot, L. Gemma 3 technical report, 2025. URL <https://arxiv.org/abs/2503.19786>.
- Thapa, R., Kjaer, M. R., He, B., Covert, I., Moore IV, H., Hanif, U., Ganjoo, G., Westover, M. B., Jennum, P., Brink-Kjaer, A., et al. A multimodal sleep foundation model for disease prediction. *Nature Medicine*, pp. 1–11, 2026.
- Vaswani, A., Shazeer, N., Parmar, N., Uszkoreit, J., Jones, L., Gomez, A. N., Kaiser, L., and Polosukhin, I. Attention is all you need, 2023. URL <https://arxiv.org/abs/1706.03762>.
- Wagner, P., Strodthoff, N., Boussejot, R.-D., Samek, W., and Schaeffter, T. PTB-XL, a large publicly available electrocardiography dataset. *PhysioNet*, November 2022. doi: 10.13026/kfzx-aw45. URL <https://doi.org/10.13026/kfzx-aw45>. Version 1.0.3.
- Wang, R., Chen, F., Chen, Z., Li, T., Harari, G., Tignor, S., Zhou, X., Ben Zeev, D., and Campbell, A. T. Studentlife: Assessing mental health, academic performance and behavioral trends of college students using smartphones. In *Proceedings of the 2014 ACM International Joint Conference on Pervasive and Ubiquitous Computing*, New York, NY, USA, 2014. Association for Computing Machinery. doi: 10.1145/2632048.2632054.
- Wang, T. and Isola, P. Understanding contrastive representation learning through alignment and uniformity on the hypersphere, 2022. URL <https://arxiv.org/abs/2005.10242>.
- Weiss, G. WISDM Smartphone and Smartwatch Activity and Biometrics Dataset. UCI Machine Learning Repository, 2019. DOI: <https://doi.org/10.24432/C5HK59>.
- Wilcoxon, F. Individual comparisons by ranking methods. *Biometrics Bulletin*, 1(6):80–83, 1945. doi: 10.2307/3001968.
- Wimmer, C. and Rekabsaz, N. Leveraging vision-language models for granular market change prediction, 2023. URL <https://arxiv.org/abs/2301.10166>.
- Woo, G., Liu, C., Kumar, A., Xiong, C., Savarese, S., and Sahoo, D. Unified training of universal time series forecasting transformers, 2024. URL <https://arxiv.org/abs/2402.02592>.
- Xie, Z., Li, Z., He, X., Xu, L., Wen, X., Zhang, T., Chen, J., Shi, R., and Pei, D. Chatts: Aligning time series with llms via synthetic data for enhanced understanding and reasoning. *arXiv preprint arXiv:2412.03104*, 2024.
- Xu, M. A., Narayanswamy, G., Ayush, K., Spathis, D., Liao, S., Tailor, S. A., Metwally, A., Heydari, A. A., Zhang, Y., Garrison, J., et al. Lsm-2: Learning from incomplete wearable sensor data. *arXiv preprint arXiv:2506.05321*, 2025.
- Yang, A., Yang, B., Hui, B., Zheng, B., Yu, B., Zhou, C., Li, C., Li, C., Liu, D., Huang, F., Dong, G., Wei, H., Lin, H., Tang, J., Wang, J., Yang, J., Tu, J., Zhang, J., Ma, J., Yang, J., Xu, J., Zhou, J., Bai, J., He, J., Lin, J., Dang, K., Lu, K., Chen, K., Yang, K., Li, M., Xue, M., Ni, N., Zhang, P., Wang, P., Peng, R., Men, R., Gao, R., Lin, R., Wang, S., Bai, S., Tan, S., Zhu, T., Li, T., Liu, T., Ge, W., Deng, X., Zhou, X., Ren, X., Zhang, X., Wei, X., Ren, X., Liu, X., Fan, Y., Yao, Y., Zhang, Y., Wan, Y., Chu, Y., Liu, Y., Cui, Z., Zhang, Z., Guo, Z., and Fan, Z. Qwen2 technical report, 2024. URL <https://arxiv.org/abs/2407.10671>.
- Yu, J., Wang, Z., Vasudevan, V., Yeung, L., Seyedhosseini, M., and Wu, Y. Coca: Contrastive captioners are image-text foundation models, 2022. URL <https://arxiv.org/abs/2205.01917>.
- Zellers, R., Bisk, Y., Schwartz, R., and Choi, Y. Swag: A large-scale adversarial dataset for grounded common-sense inference, 2018. URL <https://arxiv.org/abs/1808.05326>.
- Zhang, T., Kishore, V., Wu, F., Weinberger, K. Q., and Artzi, Y. Bertscore: Evaluating text generation with bert, 2020. URL <https://arxiv.org/abs/1904.09675>.
- Zhang, X., Zhao, Z., Tsiligkaridis, T., and Zitnik, M. Self-supervised contrastive pre-training for time series via time-frequency consistency, 2022. URL <https://arxiv.org/abs/2206.08496>.
- Zhang, Y., Ayush, K., Qiao, S., Heydari, A. A., Narayanswamy, G., Xu, M. A., Metwally, A. A., Xu, S., Garrison, J., Xu, X., Althoff, T., Liu, Y., Kohli, P., Zhan, J., Malhotra, M., Patel, S., Mascolo, C., Liu, X., McDuff, D., and Yang, Y. Sensorlm: Learning the language of wearable sensors, 2025. URL <https://arxiv.org/abs/2506.09108>.

A. Datasets

We thank the prior work that collected and open-sourced the datasets used in this work, and we summarize it again below for the convenience of future researchers. We provide the details of the non-overlapping pretraining and downstream datasets below.

A.1. Pretraining Dataset

Inspired by SensorLM (Zhang et al., 2025), we automatically generate hierarchical captions (i.e., statistical, structural, semantic) of each multivariate sensor signal. The domain distribution of this sensor-paired dataset is shown in Table A.1. We open-source this large dataset to support future research on sensor–language models, and we also release the caption generation pipeline for creating large-scale sensor–language datasets.

Table 7. Category distribution.

	Health	Synthetic	Web	Nature	Energy	IoT	Environment	Transport
# of Samples	237050	105085	67865	32358	2743	2611	1082	28
Percent (%)	52.82	23.41	15.12	7.21	0.61	0.58	0.24	0.01
Sources	(Liu et al., 2024) (Luo et al., 2025) (Chan et al., 2024)	(Xie et al., 2024)	(Liu et al., 2024)					

A.2. Downstream Dataset

Table 8. Evaluation dataset details.

Dataset	Sensor	# Samples (Train \ Test)	Freq.	# Cls	Label Names
WISDM (Weiss, 2019)	Accelerometer X, Y, Z	22396 / 5600	30Hz	18	Catch, Chips, Clap, Dribble, Drink, Fold, Jog, Kick, Pasta, Sandwich, Sit, Soup, Stair, Stand, Teeth, Type, Walk, Write
UCI-HAR (Reyes-Ortiz et al., 2013)	Accelerometer X, Y, Z Gyroscope X, Y, Z	1847 / 793	50Hz	5	Lay, Sit, Stand, Walk, Walking Upstairs, Walking Downstairs, Transition
PPG-CVA (Stroke) (Liang et al., 2018)	PPG	525 / 132	65Hz	2	Normal, Stroke
PPG-DM (Diabetes) (Liang et al., 2018)	PPG	522 / 135	65Hz	2	Normal, Diabetes
PPG-HTN (Hypertension) (Liang et al., 2018)	PPG	525 / 132	65Hz	4	Normal, Pre-hypertension, Stage-1, Stage-2
Sleep Stage (Sleep stage) (Kemp et al., 2000)	EEG-Fpz-Cz, EEG-Pz-Oz	33599 / 8709	100Hz	5	Light spindle, Light, Deep, REM, Wake
PTB-XL (Heart cond.) (Wagner et al., 2022)	12-lead ECG	11320 / 1650	100Hz	5	Normal ECG, Myocardial Infarction, ST/T Change, Conduction Disturbance, Hypertrophy

Dataset	Sensor	# Samples (Train \ Test)	Freq.	# Cls	Label Names
WESAD (Schmidt et al., 2018)	Chest Acc. X, Y, Z Chest ECG, EMG, EDA, Temp, Resp, Wrist Acc. X, Y, Z, Wrist BVP, EDA	882 / 223	700Hz	3	Neutral, Amusement, Stress
StudentLife (Wang et al., 2014)	Activity, Audio, Conversation, Phone Charge, Phone Lock, Time to deadline, Day of the week, Exam period, Sleep rating, Sleep duration	1074 / 109	Minute	3	Normal, Medium Stress, High Stress
AsphaltObstacles (Souza, 2018)	Acceleration magnitude	390 / 391	100Hz	4	Raised crosswalk, Raised markers, Speed bump, Vertical patch
Beijing AQI (Chen, 2017)	dew-point temperature, windspeed, PM25, PM10, NO2, SO2, CO	1168 / 293	Hour	4	Good, Moderate, Unhealthy for sensitive groups, Unhealthy, Hazardous

B. Pretraining Dataset Scaling

Table 9 illustrates the scaling behavior of SLIP across different data regimes. Consistent with the scaling laws observed in the original CLIP work, our results demonstrate that retrieval performance benefits significantly more from large-scale data than classification. While classification accuracy remains relatively stable—dropping only 2.88% when scaling down from 1.7B to 0.3B samples—retrieval performance collapses by 17.72%. This follows the intuition from Radford et al. (2021) that while coarse semantic categories can be learned from limited samples, the construction of a high-fidelity, shared latent space requires the "density" of a massive dataset. Large-scale pretraining is essential for the model to learn the fine-grained nuances necessary to distinguish between similar sensor-text pairs in a global retrieval space, suggesting SLIP’s greater potential with the current growing size of datasets.

Table 9. Effect of Pretraining Dataset Size

Model	Cls. Avg	Δ	Retrieval	Δ	QA	Δ
Ours (1.7 B)	77.14		39.36		64.83	
0.8 B	75.23	(-1.91)	27.09	(-12.27)	56.83	(-8)
0.3 B	74.26	(-2.88)	21.64	(-17.72)	57.79	(-7.04)

C. Implementation Details

C.1. Patch Size Heuristic

Since we are performing joint training on datasets with varying sensor resolutions and sequence lengths, we define a frequency-based patch size heuristic following (Woo et al., 2024). We incorporate a broader range of window sizes to ensure that the number of tokens per sample remains roughly consistent across diverse datasets, thereby minimizing the computational overhead caused by excessive padding. The patch sizes are assigned based on data frequency as follows:

- **Daily:** 16, 32
- **Hourly:** 6, 8, 16, 24, 32, 64
- **Minute-level:** 16, 24, 128
- **Second-level:** 4, 6, 8, 12, 16, 20, 25, 32, 64, 128

C.2. Pretraining Implementation Details

We pretrain for 40 epochs with batch size 72 on 4 NVIDIA H200 GPUs using AdamW (Loshchilov & Hutter, 2019) (weight decay = 0.05). The learning rate is warmed up to $2e^{-4}$ over 80k iterations and cosine-decayed to $1e^{-7}$. Sensor augmentations are disabled during pretraining to preserve sensor–text alignment, but standard augmentations (jittering, scaling, time flipping) are applied during supervised finetuning (Zhang et al., 2025). Additional implementation details are in the codebase.

C.3. Downstream Evaluation Details

Following the standard transfer learning evaluation protocol from prior work (He et al., 2021), we did not perform hyperparameter search (i.e. learning rate or weight decay). All models were frozen, and only a randomly initialized linear classifier was trained for 50 epochs with 5 warmup epochs using the AdamW optimizer, a base learning rate of 0.01, and a weight decay of 0.05. Supervised finetuning hyperparameter details are shown in Table 10.

Table 10. Hyperparameters used in the supervised finetuning experiment.

Hyperparameter	TSQA	HAR-CoT	Sleep-CoT	ECG-QA-CoT	M4 Caption
Optimizer	AdamW (Loshchilov & Hutter, 2019)				
Gradient clip	1.0				
LR decay schedule	Cosine Schedule Decaying to $1e^{-7}$				
Train Epoch	4	4	10	4	4
Train batch size	64	64	32	32	64
Warm up epochs	1	1	1	1	1
Weight decay rate	0.05	0.05	0.05	0.05	0.05

Table 11. Pairwise Wilcoxon results. SLIP compared with each baseline.

Eval	modelA	modelB	p_value	significant
LP	SLIP _{Base}	Stat Feat	0.000977	True
	SLIP _{Base}	SimMTM	0.000977	True
	SLIP _{Base}	TFC	0.000977	True
	SLIP _{Base}	Sundial Base	0.000977	True
	SLIP _{Base}	Normwear	0.001953	True
	SLIP _{Base}	Chronos2	0.001953	True
	SLIP _{Base}	Chronos	0.041992	True
	SLIP _{Base}	ChatTS	0.000977	True
ZS	SLIP _{Base}	Normwear	0.24	False

D. Statistical Comparisons

Table 11 reports pairwise Wilcoxon signed rank tests (Demšar, 2006; Wilcoxon, 1945) comparing SLIP with each baseline across the 11 datasets, using paired per-dataset results computed from Table 13. In the linear probing setting, SLIP differs from every baseline at the 0.05 level. In the zero-shot retrieval setting, SLIP versus Normwear is not significant, which is consistent with Normwear showing stronger alignment on the diagnosis tasks. We do not report statistical tests for the supervised finetuning experiment because there are fewer than five datasets, following the guidance in (Demšar, 2006).

E. Supplementary Results

Table 12. Additional F1 score metric. Linear-probing (LP) and zero-shot (ZS) performance across 11 datasets.

Eval	Model	WISDM	UCIHAR	Stroke	Diabetes	Hypertension	Sleep Stage	Heart Cond.	WESAD	StudentLife	Obstacles	Beijing AQI	Average
LP	Stat Feat	72.03	84.18	47.41	45.12	26.85	66.41	39.12	47.81	42.46	80.98	36.86	53.57
	SimMTM	42.93	69.13	47.20	31.35	45.12	28.68	17.17	54.56	35.86	75.85	37.32	44.11
	TFC	54.60	64.20	47.62	45.12	23.86	33.08	24.50	23.60	25.11	47.40	23.44	37.50
	NormWear	70.60	76.88	52.30	44.90	32.99	72.25	47.52	63.02	32.24	82.82	48.58	56.74
	Chronos2	74.43	81.41	47.41	43.28	34.96	73.83	35.76	57.26	26.35	78.83	25.28	52.62
	Chronos	80.06	81.73	47.35	57.70	35.54	66.07	48.89	51.72	28.17	74.61	61.17	57.47
	Sundial Base	80.90	41.64	47.62	45.12	13.54	51.18	30.53	36.85	38.41	67.68	36.15	44.51
	ChatTS	75.36	57.31	47.62	45.12	13.93	69.70	42.36	57.31	36.19	76.12	29.85	50.08
	SLIP	81.87	84.58	54.74	51.71	39.59	70.98	48.67	71.84	40.62	84.32	45.32	61.17
Zero-shot Retrieval	NormWear	0.48	3.89	47.20	45.12	13.48	11.24	5.37	9.49	20.09	14.00	1.83	15.65
	SLIP	5.47	13.80	46.34	45.19	17.15	29.22	5.36	46.02	24.97	15.33	13.81	23.88

Table 13. Additional supplementary results. Linear-probing (LP) and zero-shot (ZS) retrieval performance across 11 datasets, reported as mean and standard deviation over 5-fold evaluation with different random seeds.

Eval	Model	WISDM	UCIHAR	Stroke	Diabetes	Hypertension	Sleep Stage	Heart Cond.	WESAD	StudentLife	Obstacles	Beijing AQI
LP	Stat Feat	77.14 ± 0.25	85.62 ± 0.38	90.15 ± 0.00	82.22 ± 0.00	37.73 ± 1.30	77.33 ± 0.024	60.99 ± 0.33	68.52 ± 0.77	48.26 ± 1.37	81.69 ± 0.80	68.81 ± 0.51
	SimMTM	33.76 ± 0.08	70.52 ± 0.24	89.39 ± 0.00	82.22 ± 0.00	37.88 ± 1.07	41.76 ± 0.07	55.90 ± 0.08	62.51 ± 0.46	50.64 ± 0.69	36.37 ± 0.98	71.26 ± 0.26
	TFC	44.11 ± 0.11	59.95 ± 0.13	89.85 ± 0.61	80.74 ± 0.47	40.00 ± 0.57	44.88 ± 0.05	58.11 ± 0.25	55.43 ± 0.46	43.67 ± 1.70	33.66 ± 0.62	45.60 ± 0.46
	Normwear	70.82 ± 0.03	79.37 ± 0.32	90.45 ± 0.61	82.37 ± 0.30	40.45 ± 1.13	82.92 ± 0.18	69.53 ± 0.07	80.27 ± 0.49	49.17 ± 1.24	83.38 ± 0.32	74.40 ± 0.38
	Chronos2	75.18 ± 0.07	75.38 ± 0.51	87.12 ± 0.96	73.33 ± 3.18	38.79 ± 0.88	83.74 ± 0.14	61.20 ± 0.19	67.26 ± 0.75	47.89 ± 0.69	84.14 ± 0.23	51.74 ± 0.63
	Chronos	81.19 ± 0.13	84.04 ± 0.30	88.48 ± 2.00	80.59 ± 1.36	45.30 ± 0.88	76.69 ± 0.14	73.27 ± 0.18	66.46 ± 0.18	49.54 ± 1.00	75.45 ± 0.28	80.48 ± 0.14
	Sundial Base	41.39 ± 0.12	55.84 ± 0.29	77.27 ± 0.83	72.00 ± 5.03	37.73 ± 3.16	70.19 ± 0.14	61.26 ± 0.12	59.64 ± 0.40	47.53 ± 2.20	68.04 ± 0.23	67.85 ± 0.26
	ChatTS	75.66 ± 0.00	56.24 ± 0.00	90.91 ± 0.00	82.22 ± 0.00	44.70 ± 0.00	80.65 ± 0.08	67.93 ± 0.21	77.04 ± 0.18	50.28 ± 0.90	77.75 ± 0.65	61.23 ± 1.84
	SLIP	82.28 ± 0.10	85.67 ± 0.26	91.36 ± 0.67	83.11 ± 0.55	47.58 ± 0.57	82.62 ± 0.09	71.59 ± 0.19	81.79 ± 0.61	54.31 ± 1.58	85.32 ± 0.35	76.66 ± 0.27
Zero-shot Retrieval	Normwear	3.91 ± 0.66	12.98 ± 2.15	89.40 ± 3.74	82.22 ± 7.18	36.38 ± 8.38	39.09 ± 0.73	15.52 ± 1.26	16.58 ± 6.43	43.12 ± 13.02	24.30 ± 2.03	2.40 ± 2.34
	SLIP	7.45 ± 0.14	27.26 ± 0.46	90.91 ± 0.00	75.56 ± 2.65	35.76 ± 0.30	34.58 ± 0.17	16.08 ± 0.19	40.45 ± 0.87	42.02 ± 0.69	30.08 ± 0.13	22.25 ± 1.67

Table 14. Ablation Studies Linear Probing Performance. Top-1 accuracy on 11 datasets, reported as mean and standard deviation over 5-fold evaluation with different random seeds.

Model	WISDM	UCIHAR	Stroke	Diabetes	Hypertension	Sleep Stage	Heart Cond.	WESAD	StudentLife	Obstacles	Beijing AQI	All Avg
SLIP_{Base}	82.36	86.25	91.67	84.44	50.00	82.04	70.79	82.96	54.13	86.45	77.47	77.14
Contrastive-Only	79.14	85.37	90.91	84.44	40.91	81.10	68.12	82.96	50.46	84.65	74.40	74.77
Caption-Only	82.11	84.36	90.91	83.70	37.12	81.96	69.70	76.68	46.79	85.42	78.50	74.30
Random Paired	38.16	65.45	90.91	82.96	41.67	59.62	55.39	52.47	52.47	74.93	69.62	62.15
w/o FlexMLP ($p_s = 16$)	76.80	89.16	87.88	82.22	47.73	82.55	70.73	72.20	46.79	84.91	74.74	74.16
w/ Group Attention	79.45	84.36	92.42	85.19	48.48	81.67	72.12	83.41	56.88	85.94	77.47	77.04
Freeze Text Encoder	76.75	85.12	83.33	79.26	40.91	79.21	66.55	87.44	54.13	82.35	74.06	73.56
SLIP _{Small} (40M)	80.54	81.84	90.91	83.70	42.42	80.74	68.67	81.17	49.54	84.91	78.84	74.84

Table 15. Ablation Studies Zero-Shot Retrieval Performance. Top-1 accuracy on 11 datasets.

Model	WISDM	UCIHAR	Stroke	Diabetes	Hypertension	Sleep Stage	Heart Cond.	WESAD	StudentLife	Obstacles	Beijing AQI	All Avg
SLIP_{Base}	7.45	27.62	86.40	74.07	34.85	34.83	15.39	56.95	41.28	29.92	24.23	39.36
Contrastive-Only	9.50	19.67	79.55	80.74	24.24	39.05	10.97	52.47	40.37	30.18	19.11	36.90
Caption-Only	5.82	6.56	78.03	17.78	38.64	20.87	7.21	21.52	42.20	29.16	8.53	25.12
Random Paired	5.09	4.04	81.06	17.78	9.09	22.20	3.39	16.59	24.77	18.16	44.03	22.38
w/ Group Attention	8.30	27.11	84.09	82.22	36.36	26.28	26.85	52.02	44.95	24.04	19.11	39.21
w/o FlexMLP ($p_s = 16$)	5.86	13.75	90.15	59.26	29.54	29.02	8.79	40.81	30.28	30.18	45.05	34.79
Freeze Text Encoder	12.02	17.28	70.46	82.22	34.85	39.48	13.15	23.32	36.70	42.20	20.82	35.68
SLIP _{Small} (40M)	11.27	9.84	43.18	32.59	36.36	33.01	14.67	22.42	20.18	20.46	49.83	26.71

Table 16. Ablation Studies SFT performance. Top-1 accuracy on four sensor QA benchmarks.

Model	TSQA	HAR-CoT	Sleep-CoT	ECG-QA-CoT	Avg
SLIP_{Base}	83.60	64.35	74.19	37.18	64.83
Caption-Only	76.65	49.16	69.14	34.07	57.26
Contrastive-Only	75.75	48.57	29.57	38.21	48.03
Random Paired	57.73	27.93	21.51	33.16	35.08
w/ Group Attention	65.42	60.41	69.14	37.05	58.01
w/o FlexMLP ($p_s = 16$)	76.65	61.66	69.03	38.17	61.38
Freeze Text Encoder	85.54	47.00	61.18	34.62	57.09
SLIP _{Small} (40M)	75.60	50.58	64.09	25.70	53.99

Table 17. Token usage. Average input tokens for different input formulations across 11 datasets in zero-shot classification.

Model	WISDM	UCIHAR	Stroke	Diabetes	Hypertension	Sleep Stage	Heart Cond.	WESAD	StudentLife	Obstacles	Beijing AQI	Average
SLIP_{Base}	66	246	30	55	85	257	53	738	1452	109	302	308.45
NormWear	1308	1730	380	380	382	8665	8753	56290	20680	1054	2828	9313.64
LLM-Text (Gemma-3-270M-IT)	5562	7336	1717	1713	1728	38696	37103	234156	86546	4523	12234	39210.36
VLM-Images (Gemma-3-4B-IT)	409	368	347	343	358	377	435	360	375	363	359	372.18
ChatTS (8B)	339	576	125	125	125	920	1598	5786	2504	184	745	1184.27

F. Additional Details on Uniformity and Alignment

Following (Wang & Isola, 2022), the key idea is to view contrastive learning as balancing two geometric effects in the embedding space. Alignment measures whether a model pulls together embeddings of positive pairs that should represent the same underlying content, while uniformity measures whether embeddings of different samples remain spread out on the unit hypersphere instead of collapsing. In their original image setting, a positive pair is two augmented views of the same image, and negatives are views from other images in the batch. Good representations therefore require low alignment loss, meaning the two views of the same image land close, while also maintaining good uniformity, meaning the whole set of image embeddings does not crowd into a small region.

In sensor language contrastive learning, the same definitions apply after replacing the notion of a positive pair. Here, the positive pair is a matched sensor segment x and its paired text description y , and negatives are mismatched sensor text pairs (x_i, y_j) with $i \neq j$. Alignment then becomes a direct measure of sensor to language coupling: if the representation is truly shared, embeddings of matched sensor and text should be close. Namely,

$$\mathcal{L}_{\text{align}} \triangleq \mathbb{E}_{(x,y) \sim \mathcal{D}^+} [\|f(x) - f(y)\|_2^\alpha], \quad \alpha > 0.$$

Uniformity becomes a check against collapse within each modality: sensor embeddings should remain spread across the sphere so different signals are distinguishable, and text embeddings should remain spread so different descriptions are distinguishable. The uniformity loss is defined as the logarithm of the average pairwise Gaussian potential:

$$\begin{aligned} \mathcal{L}_{\text{unif}}(f; t) &\triangleq \log \mathbb{E}_{x,y \sim \mathcal{D}} [G_t(x, y)] \\ &= \log \mathbb{E}_{x,y \sim \mathcal{D}} \left[e^{-t\|f(x)-f(y)\|_2^2} \right], \quad t > 0. \end{aligned}$$

This is especially useful for sensor data because many windows can be similar and the model can otherwise reduce loss by relying on the stronger text branch, so tracking sensor uniformity alongside cross modal alignment helps distinguish true cross modal alignment from a degenerate solution. Altogether, we will measure sensor-language alignment, sensor uniformity, and text uniformity with implementation in Alg. 2.

Algorithm 2 PyTorch style code for alignment and uniformity.

```

1
2 import torch
3 import torch.nn.functional as F
4
5 # bsz: batch size (number of positive pairs)
6 # d: latent dim
7 # x: Tensor, shape=(bsz, d)  sensor embeddings
8 # y: Tensor, shape=(bsz, d)  text embeddings
9
10 x = F.normalize(x, dim=1)
11 y = F.normalize(y, dim=1)
12
13 def lalign(x, y, alpha=2):
14     return (x - y).norm(dim=1).pow(alpha).mean()
15
16 def lunif(x, t=2):
17     sq_pdist = torch.pdist(x, p=2).pow(2)
18     return sq_pdist.mul(-t).exp().mean().log()
19
20 alignment_loss = lalign(x, y)
21 text_uniformity_loss = lunif(y)
22 sensor_uniformity_loss = lunif(x)

```

G. Prompt Examples

```
Prompt template (MCQ, UCIHAR, Sensor as Text)
<bos><start_of_turn>user
You are a precise sensor data classifier. You must respond with only a single letter
(A, B, C, D...) and nothing else. Never explain your reasoning.
Classify the following accelerometer and gyroscope data in meters per second squared as
daily activities:
Acc_x: -0.01, -0.01, -0.01, -0.01, ...
Acc_y: -0.01, -0.01, -0.01, -0.01, ...,
Gyr_x: 0.21, 0.21, 0.21, 0.21, ...
Options:
A. laying
B. sitting
C. standing
D. transition
E. walking
F. walking downstairs
G. walking upstairs
Task: Output the letter of the correct activity.
Answer:<end_of_turn>
<start_of_turn>model
```

Figure 5. Example MCQ template used for Gemmani-4b-IT and Gemmani-270M-IT.

Prompt template (MCQ, Beijing_AQI, Sensor as Text)

```

<bos><start_of_turn>user
You are a precise sensor data classifier. You must respond with only a single letter
(A, B, C, D...) and nothing else. Never explain your reasoning.
Classify the following environmental time series into an AQI level.
dew point temperature: 1.10, 1.21, 1.16, ...
windspeed (m/s): -0.43, -1.39, -0.34, ...
PM10 sub index: -0.23, -0.04, -0.10, ...
NO2 sub index: -0.30, 0.20, -0.27, ...
SO2 sub index: -0.64, -0.59, -0.70, ...

Options:
A. Good
B. Hazardous
C. Moderate
D. Unhealthy
E. Unhealthy for sensitive groups

Task: Output the letter of the correct activity.
Answer:<end_of_turn>
<start_of_turn>model
    
```

Figure 6. Example MCQ template used for Gemmani-4b-IT and Gemmani-270M-IT.

Prompt template (MCQ, UCIHAR, Sensor as Image)

```

<bos><start_of_turn>user
You are a precise sensor data classifier. You
must respond with only a single letter (A, B,
C, D...) and nothing else. Never explain your
reasoning.
Classify the following accelerometer and gyroscope
data in meters per second squared as daily
activities:
<start_of_image>
Options:
A. laying
B. sitting
C. standing
D. transition
E. walking
F. walking downstairs
G. walking upstairs

Task: Output the letter of the correct activity.
Answer:<end_of_turn>
<start_of_turn>model
    
```

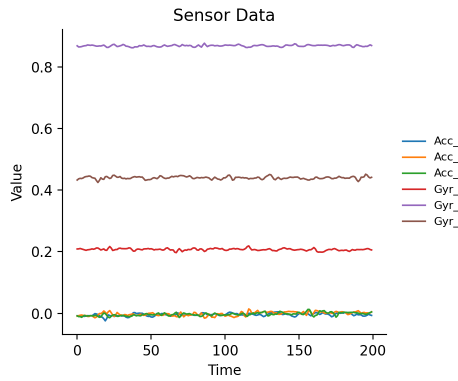


Figure 7. Example MCQ prompt template used for using sensor as images. The sensor segment is rendered as an image and provided to the VLM using the <start_of_image> token.

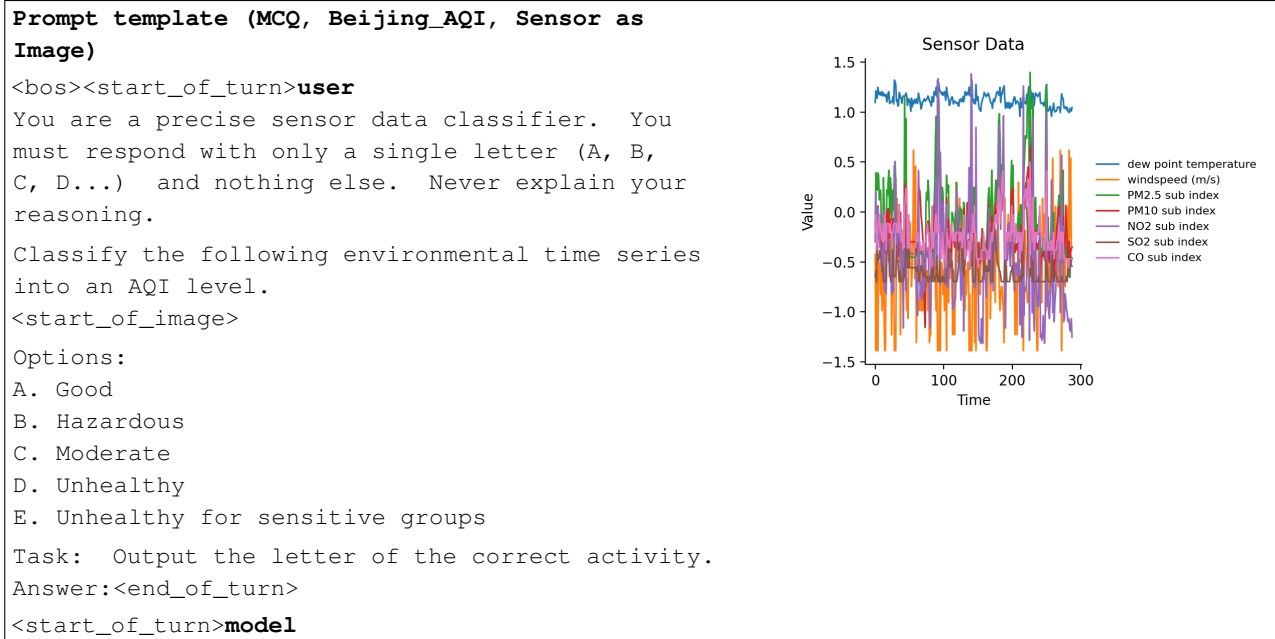


Figure 8. Example MCQ prompt template used for using sensor as images. The sensor segment is rendered as an image and provided to the VLM using the `<start_of_image>` token.

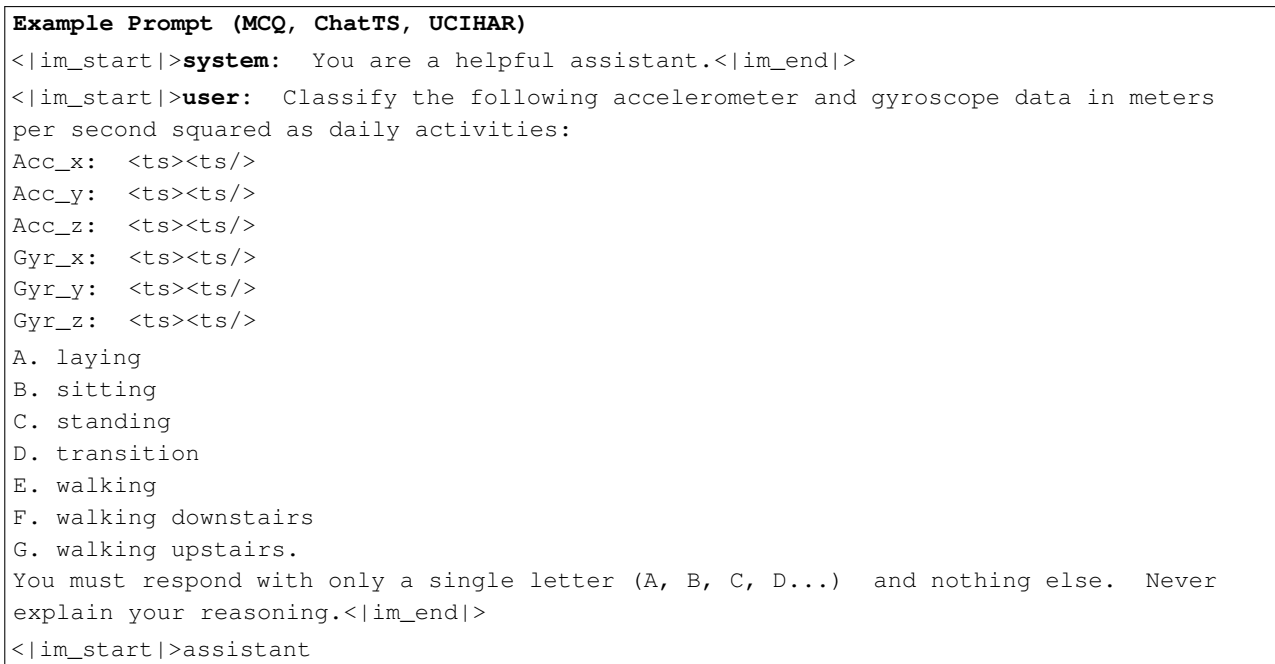


Figure 9. Example MCQ template used for ChatTS. Numerical sensor input will be process into tokens and replace `<ts><ts/>` by the ChatTS Model.

```
Prompt template (MCQ, ChatTS, Beijing_AQI)
<|im_start|>system
You are a helpful assistant.<|im_end|>
<|im_start|>user
Classify the following environmental time series into an AQI level.
dew point temperature: <ts><ts/>
windspeed (m/s): <ts><ts/>
PM2.5 sub index: <ts><ts/>
PM10 sub index: <ts><ts/>
NO2 sub index: <ts><ts/>
SO2 sub index: <ts><ts/>
CO sub index: <ts><ts/>
A. Good
B. Hazardous
C. Moderate
D. Unhealthy
E. Unhealthy for sensitive groups.
You must respond with only a single letter (A, B, C, D...) and nothing else. Never
explain your reasoning.<|im_end|>
<|im_start|>assistant
```

Figure 10. Example MCQ template used for ChatTS. Numerical sensor input will be process into tokens and replace <ts><ts/> by the ChatTS Model.

H. Additional Examples of Question Answering

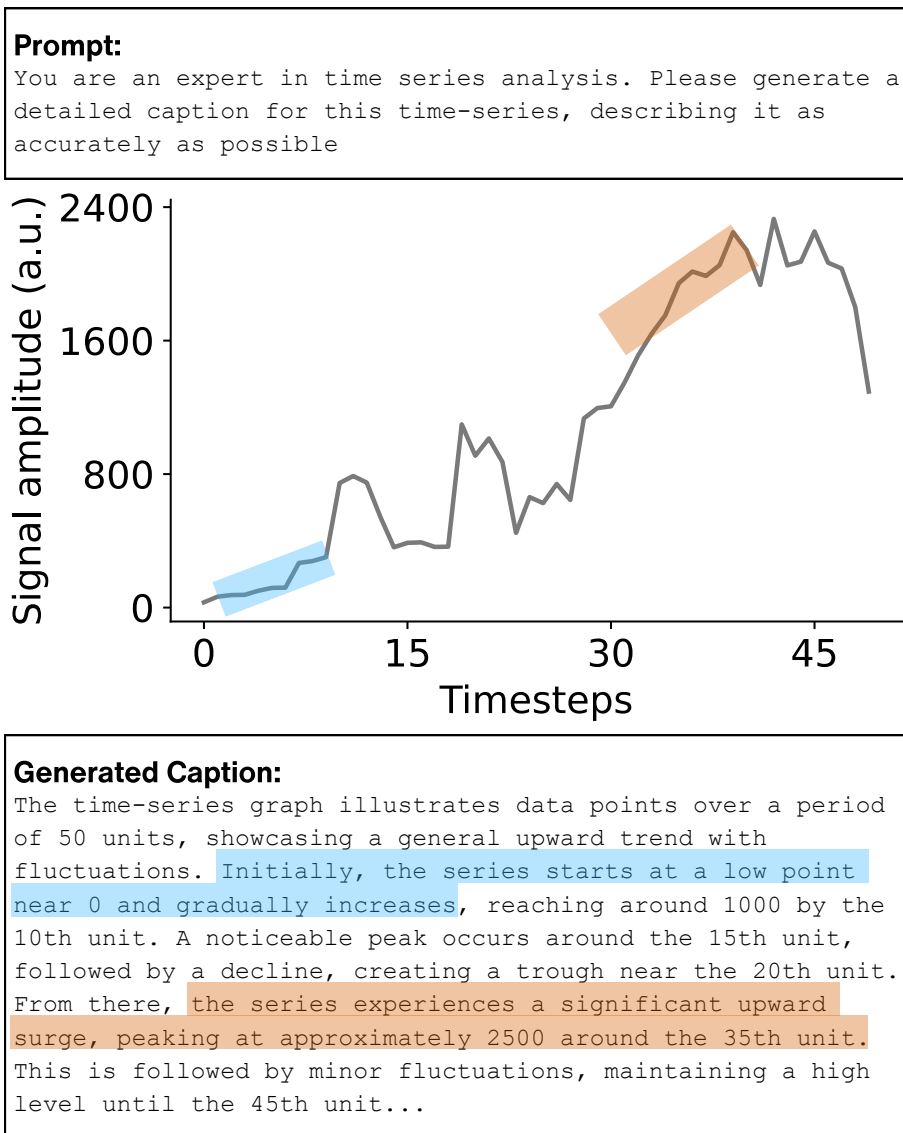
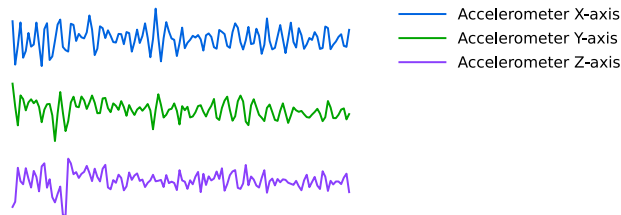


Figure 11. A qualitative example of sensor captioning from the M4 dataset. Highlighted segments denote salient local trends referenced in the generated caption.

Prompt:
 Instructions:
 - Begin by analyzing the time series without assuming a specific label.
 - Think step-by-step about what the observed patterns suggest regarding movement intensity and behavior.
 - Write your rationale as a single, natural paragraph – do not use bullet points, numbered steps, or section headings.
 - Do ****not**** mention any class label until the final sentence.

Possible activity labels are:
 biking, lying, running, sitting, standing, walking, walking_down, walking_up.

- Make sure that your last word is the answer. You **MUST** end your response with "Answer: "



Prediction:
Rationale: The accelerometer data over the 2.56 second window shows significant variability across all three axes, indicating substantial movement. The **X-axis exhibits frequent peaks and troughs, suggesting lateral or forward-backward motion** that is consistent with dynamic activity. The **Y-axis also displays fluctuations**, though they are less pronounced, which might indicate less vertical movement or tilt. **The Z-axis shows moderate variability**, which could be associated with subtle changes in height or orientation. The overall pattern of the data **suggests a continuous and rhythmic motion, likely involving repetitive cycles** of movement. The presence of such variability and intensity across all axes is more characteristic of an activity involving consistent motion and balance adjustments rather than a static or minimal movement scenario. Therefore, the observed patterns are more aligned with the activity of biking. **Answer: biking.**

Ground Truth:
 The accelerometer data over the 2.56 second window shows significant variability across all three axes, indicating substantial movement. The X-axis and Y-axis **exhibit frequent fluctuations with both positive and negative accelerations**, suggesting dynamic motion rather than a static position. The **Z-axis also shows variability, although with slightly less amplitude**, which could indicate vertical movement or changes in elevation. The overall pattern suggests a **repetitive, rhythmic motion consistent with a cycling activity**, where the body experiences continuous motion due to pedaling and shifts in balance. These characteristics are less likely to be observed in a stationary activity, which would typically show minimal changes in acceleration. Therefore, the observed patterns are more indicative of an active movement rather than stillness. **Answer: biking.**

Figure 12. A qualitative example of sensor question answering from the Har-CoT dataset.

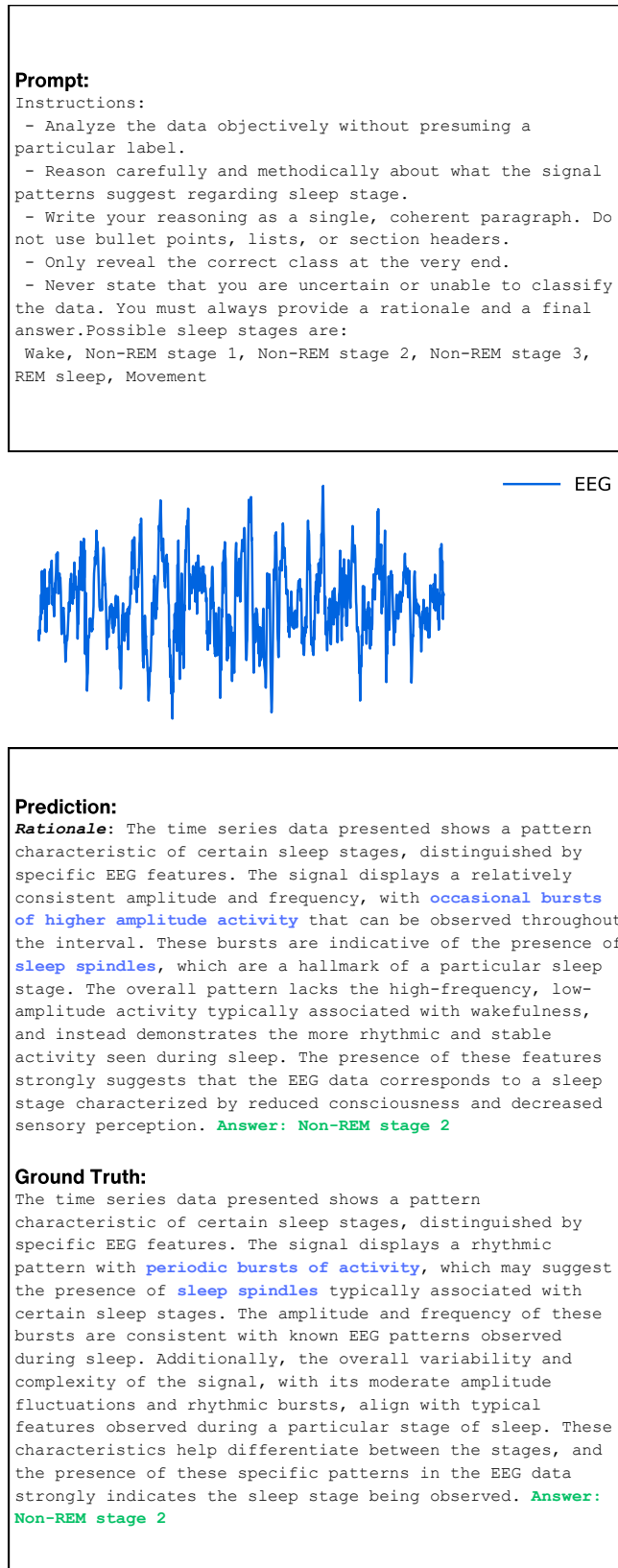


Figure 13. A qualitative example of sensor question answering from the Sleep-CoT dataset.

Prompt:

Instructions:

Given the following definitions: Constant volatility: The time series shows relatively consistent fluctuation magnitude throughout the period. Increased volatility: The time series shows a rise in the magnitude of fluctuation over time. Decreased volatility: The time series shows a reduction in the magnitude of fluctuations over time. Select one of the following answers that best describes the provided time series:

- (a) This time series has a constant volatility.
- (b) This time series has an increased volatility.
- (c) This time series has a decreased volatility.

Only answer (a), (b), or (c). Predict the Volatility Answer:



Prediction: C

Ground Truth: C

Figure 14. A qualitative example of Multiple Choice Question from the TSQA dataset.

Prompt:
 Clinical Context: 75-year-old male patient. 12-lead ECG. clinical recording. recorded with AT-6 C S.S. Signal quality: baseline drift noted, static noise present, burst noise present, electrode artifacts present. extra beats detected during recording. pacemaker present.

Your task is to examine the ECG signal and answer the following medical question:

Question: Which diagnostic symptom does this ECG show, myocardial infarction in anterior leads or myocardial infarction in anteroseptal leads, excluding uncertain symptoms?

Instructions:
 - Begin by analyzing the time series without assuming a specific answer.
 - Think step-by-step about what the observed patterns suggest regarding the cardiac condition.
 - Write your rationale as a single, natural paragraph
 - do not use bullet points, numbered steps, or section headings.
 - Do **not** mention any final answer until the very end.
 - Consider the ECG morphology, intervals, and any abnormalities that relate to the question.
 Based on your analysis of the ECG data, select your answer from the following options:
 complete left bundle branch block,
 complete right bundle branch block,
 digitalis effect, first degree av block,
 ...
 ...
 ...
 - Make sure that your last word is the answer. You **MUST** end your response with "Answer: "

Prediction:
 Side analysis for the 12-lead ECG of this 75-year-old male patient. The presence of a pacemaker and various artifacts such as baseline drift, static noise, burst noise, and electrode artifacts complicate the interpretation. However, focusing on the cardiac patterns, the leads V1 through V4, which represent the anteroseptal region, should be closely examined for signs of **myocardial infarction**. In these leads, significant ST-segment elevation or pathological Q waves would indicate myocardial infarction. The presence of extra beats may suggest arrhythmias, but the primary concern is the identification of ischemic changes. The absence of significant changes in the inferior leads (II, III, aVF) and **the lack of reciprocal changes in the anterior leads (V1-V3) further support the localization of the infarction to the anteroseptal region**. Given these observations, the ECG findings are consistent with myocardial infarction in the anteroseptal leads. Answer: myocardial infarction in anteroseptal leads. The ECG shows significant changes in the anteroseptal leads, specifically V1 to V4, which are indicative of myocardial infarction in this region. Answer: **myocardial infarction in anteroseptal leads.**

Ground Truth:
 The ECG shows evidence of myocardial infarction, particularly focusing on the anterior leads. In this recording, the presence of ST-segment elevation in leads V1 through V4 is indicative of an anterior **myocardial infarction**. These leads correspond to the anterior wall of the heart, which is typically affected in such cases. **The baseline drift and noise present in the recording do not obscure the clear elevation of the ST segments in these leads.** The presence of a pacemaker and extra beats does not alter the interpretation of the ST-segment changes, which are crucial in diagnosing myocardial infarction. The absence of significant changes in the lateral leads (I, aVL, V5, V6) further supports the localization of the infarction to the anterior region rather than a lateral or subendocardial injury. Therefore, based on the observed patterns, the ECG is consistent with myocardial infarction in the anterior leads. Answer: **myocardial infarction in anterior leads.**

Figure 15. A qualitative failure example of sensor question answering from the ECG-QA-CoT dataset.